FOREWORD

This volume is the thirty-third of the WADD Technical Report 61-72 series describing various phases of research and development on advanced graphite materials conducted by Union Carbide Corporation, Carbon Products Division, under USAF Contract No. AF 33(616)-6915.

The work covered in this report was conducted from May 1961 through January 1963 at the Advanced Materials Laboratory of the Carbon Products Division under the management of R. M. Bushong, Director of the Advanced Materials Project and of R. C. Stroup, Manager of the Advanced Materials Laboratory.

The contract for this R&D program was initiated under Project No. 7350 "Refractory Inorganic Nonmetallic Materials," Task No. 735002, "Refractory Inorganic Nonmetallic Materials: Graphitic," Project No. 7381, Materials Application," Task No. 738102, "Materials Processes," and Project No. 7-817, "Process Development for Graphite Materials." The work was administrated by the Air Force Materials Laboratory, Research and Technology Division, Captain R. H. Wilson, L. J. Conlon, and W. P. Conrardy acting as Project Engineers.

Other volumes of WADD Technical Report 61-72 series are:

Volume I - Observations by Electron Microscopy of Dislocations in Graphite, by R. Sprague.

Volume II - Applications of Anisotropic Elastic Continuum Theory to Dislocations in Graphite, by G. B. Spence.

Volume III - Decoration of Dislocations and Low Angle Grain Boundaries in Graphite Single Crystals, by R. Bacon and R. Sprague.

Volume IV - Adaptation of Radiographic Principles to the Quality Control of Graphite, by R. W. Wallouch.

Volume V - Analysis of Creep and Recovery Curves for ATJ Graphite, by E. J. Seldin and R. N. Draper.

Volume VI - Creep of Carbons and Graphites in Flexure at High Temperature, by E. J. Seldin.

Volume VII - High-Density Recrystallized Graphite by Hot-Forming, by E. A. Neel, A. A. Kellar, and K. J. Zeitsch.

Supplement - High-Density Recrystallized Graphite by Hot-Forming, by G. L. Rowe and M. B. Carter.

Volume VIII - Electron Spin Resonance in Polycrystalline Graphite, by L. S. Singer and G. Wagoner.

Volume IX - Fabrication and Properties of Carbonized Cloth Composites, by W. C. Beasley and E. L. Piper.

Volume X - Thermal Reactivity of Aromatic Hydrocarbons, by I. C. Lewis and T. Edstrom.

Supplement - Thermal Reactivity of Aromatic Hydrocarbons, by I. C. Lewis and T. Edstrom.

Volume XI - Characterization of Binders Used in the Fabrication of Graphite Bodies, by E. de Ruiter, A. Halleux, V. Sandor, and H. Tschamler.

Supplement - Characterization of Binders Used in the Fabrication of Graphite Bodies, by E. de Ruiter, J. F. M. Oth, V. Sandor and H. Tschamler.

Volume XII - Development of an Improved Large-Diameter Fine-Grain Graphite for Aerospace Applications, by C. W. Waters and E. L. Piper.

Supplement - Development of an Improved Large-Diameter Fine-Grain Graphite for Aerospace Applications, by R. L. Racicot and C. W. Waters.

Volume XIII - Development of a Fine-Grain Isotropic Graphite for Structural and Substrate Applications, by R. A. Howard and E. L. Piper.

Supplement - Development of a Fine-Grain Isotropic Graphite for Structural and Substrate Applications, by R. A. Howard and R. L. Racicot.

Volume XIV - Study of High-Temperature Tensile Properties of ZTA Grade Graphite, by R. M. Hale and W. M. Fassell, Jr.

Volume XV - Alumina-Condensed Furfuryl Alcohol Resins, by C. W. Boquist, E. R. Nielsen, H. J. O'Neil and R. E. Putcher.

Volume XVI - An Electron Spin Resonance Study of Thermal Reactions of Organic Compounds, by L. S. Singer and I. C. Lewis.

Volume XVII - Radiography of Carbon and Graphite, by T. C. Furnas, Jr. and M. R. Rosumny.

Volume XVIII - High-Temperature Tensile Creep of Graphite, by E. J. Seldin.

Volume XIX - Thermal Stresses in Anisotropic Hollow Cylinders, by Tu-Lung Weng.

Volume XX - The Electric and Magnetic Properties of Pyrolytic Graphite, by G. Wagoner and B. H. Eckstein.

Volume XXI - Arc Image Furnace Studies of Graphite, by M. R. Null and W. W. Lozier.

Volume XXII - Photomicrographic Techniques for Carbon and Graphite, by G. L. Peters and H. D. Shade.

Volume XXIII - A Method for Determining Young's Modulus of Graphite at Elevated Temperatures, by S. O. Johnson and R. B. Dull.

Volume XXIV - The Thermal Expansion of Graphite in the c-Direction by C. E. Lowell.

Volume XXV - Lamellar Compounds of Nongraphitized Petroleum Cokes, by H. F. Volk.

Volume XXVI - Physical Properties of Some Newly Developed Graphite Grades, by R. B. Dull.

Volume XXVII - Carbonization Studies of Aromatic Hydrocarbons, by I. C. Lewis and T. Edstrom.

Volume XXVIII - Polarographic Reduction of Polynuclear Aromatics, by I. C. Lewis, H. Leibecki, and S. L. Bushong.

Volume XXIX - Evaluation of Graphite Materials in a Subscale Solid-Propellant Rocket Motor, by D. C. Hiler and R. B. Dull.

Supplement - Evaluation of Graphite Materials in a Subscale Solid-Propellant Rocket Motor, by S. O. Johnson and R. B. Dull.

Volume XXX - Oxidation-Resistant Graphite-Base Composites, by K. J. Zeitsch and J. Criscione.

Volume XXXI - Impregnation of Graphite, by C. E. Waylett, M. A. Spring, and M. B. Carter.

Volume XXXII - Studies of Binder Systems for Graphite, by T. Edstrom, I. C. Lewis, R. L. Racicot, and C. F. Stout.

ABSTRACT

This report is concerned with fabrication and testing of hot-pressed (ZT) graphites made from several base stocks. Physical properties, with emphasis on porosimetry, are reported for varieties of molded and pressure-cured graphites both before and after hot pressing. A small amount of work was also done with hot pressing of extruded graphites, powders, composites, and the surfaces of formed articles. The latter process is termed surface densification.

This report has been reviewed and is approved.

W. G. RAMKE
Chief, Ceramics and Graphite Branch
Metals and Ceramics Division
AF Materials Laboratory

TABLE OF CONTENTS

LIST OF ILLUSTRATIONS

LIST OF ILLUSTRATIONS (CONT'D)

LIST OF TABLES

1. INTRODUCTION

The purpose of the work discussed in this report was to study the physical property changes made in various graphites by a hot-pressing process (ZT). The ZT process consists of heating a billet of graphite to a plastic state and compressing the billet to a volume smaller than it occupied originally. This action increases the density of the graphite and can have profound effects on its other physical properties. The hot-pressing process and the first grade of hot-pressed graphite, grade ZTA, are described in another report of this series.[1]

After experience with many hot-pressing runs, the following statements appear to be valid:

1) Good-quality graphites must be used as the starting materials to produce good-quality ZT graphites.

2) Final baking temperature (above 900°C) of the stock before hot pressing has no effect on the properties of graphite made by the ZT process.

3) Drastic hot working, or grain reorientation, degrades or destroys the stock.

4) Hot pressing has more effect on the strength properties of conventionally molded graphites than it does on pressure-cured graphites.

5) Hot pressing greatly reduces porosity in graphites.

Conclusions about and descriptions of specific materials are stated in Sections 3 through 8 of this report.

The ZT process was conceived to improve the strength, increase the bulk density, and decrease the porosity of graphite. After the first ZT materials were made, additional property changes were found.

Graphite is elemental carbon in its most stable or crystalline form. The crystal structure of graphite has layer planes of hexagonally arranged atoms which are bound tightly along the layer planes but loosely between the planes. All graphite is not the same. Artificial graphites, being made with variations in raw materials and variations in processing, are a family of materials each of which has slightly different properties from others, but some degree of anisotropy is one characteristic common to all graphites. Because of the crystalline structure and orientation of graphite, its properties along the layer planes are significantly

Manuscript released by the authors December 1963 for publication as a RTD Technical Documentary Report.

different from its properties across the layer planes. These directions are usually specified as "with grain" and "across grain", respectively.

The degree of anisotropy of graphite is influenced by the manufacturing process and by graphitization conditions; i.e., the higher the temperature and the longer the residence time, the more ordered the crystal structure of the graphite becomes. The degree of anisotropy of a graphite is often expressed as the ratio of a given property (e.g., specific resistance) in the across-grain to with-grain directions. The most anisotropic structure (in a manufactured graphite) is found in pyrolytic graphite, which may have anisotropy ratios, based on specific resistance, greater than 8,000 to 1, while there are other manufactured graphites with anisotropy ratios approaching 1 to 1 for the same property. Graphites produced by the ZT process fall between those just mentioned, having anisotropy ratios approaching 10 to 1.

Graphite is also considered a brittle material at temperatures up to about 1700°C, but above this temperature, it becomes increasingly subject to plastic deformation. At room temperature, the broken surface of a piece of graphite will display the same characteristics found in a piece of broken ceramic or concrete.

ZTA graphite has greater tensile and flexural strengths in the with-grain direction than does the base stock (ATJ graphite) from which it is made. This is attributable to the greater degree of crystal alignment imparted to ZTA. These same strengths are reduced, however, in the across-grain direction. Specific resistance, compressive strength, and CTE (coefficient of thermal expansion) are the opposite; they are decreased in the with-grain direction and increased in the across-grain direction. Grade ZTA also is more machinable than ATJ graphite; it can be machined to very close tolerances and its surface can be polished to a high luster. Another striking property of ZTA is its reduced porosity. Total mercury porosity of the raw material is reduced more than 50 per cent during hot working.

2. PROCEDURE

2.1. General Operation

In the hot-pressing process, a billet of graphite is loaded into an insulated container, the container is inserted in a hydraulic press, and the billet is heated and then compressed about 30 to 35 per cent. Since the ZT process makes use of temperatures higher than the melting point of most metals, the tooling involves careful selection of materials and special cooling and handling problems. The product billet is surrounded by high-temperature insulation which in turn is surrounded by a water-cooled jacket. The punches that contact the billet must have reasonably low thermal conductivity and must also be able to withstand the high pressures required to compress the billet. Water cooling is used on the outside and ends of the punches to keep temperatures at a moderate level. Thermal efficiency in the process is not high, and sufficient power must be made available to compensate for heat losses.[1]

2.2. Process Equipment

During the first several months that the ZT process was used, a period of many hours was required for each run. To reduce run time and to make the process more efficient, the process equipment was redesigned.

An altered cooling system (Figure 1) was used and the product and punches were packed as a separate unit to be handled intact before, during, and after processing. Instead of having a copper coil imbedded in castable, a solid cylindrical shape was used for the full length of the mold box. Water-cooling channels were run near the outside surface of the cylinder. The external dimensions of the hot-pressing assembly were such as to provide a slip fit into the cylinder. The assembly itself consisted of a graphite tube which enclosed the coke packing, product billet, and a layer of high-temperature insulation (carbon black). The graphite tube was long enough to hold the top and bottom punches, which came directly into contact with the product billet. This entire package, with the punches protruding from each end, was then placed in the cooling cylinder (between the press rams). At the end of a process run the punch ends were almost even with the ends of the graphite tube. The temperature differential from the center to the outside of the package was such that the entire assembly could be ejected easily from the press and put in a cooling tub.

The combination of cooling cylinder and process package has been used successfully for several months. Figure 1 depicts the ZT container placed in position for hot pressing. Figure 2 is a photograph of the assembly being ejected from the press after hot pressing.

2.3. Physical Testing

To determine more fully the effects of the hot-pressing process on graphite properties, and to evaluate materials for fabricating different and perhaps better ZT materials, trials were run using a number of

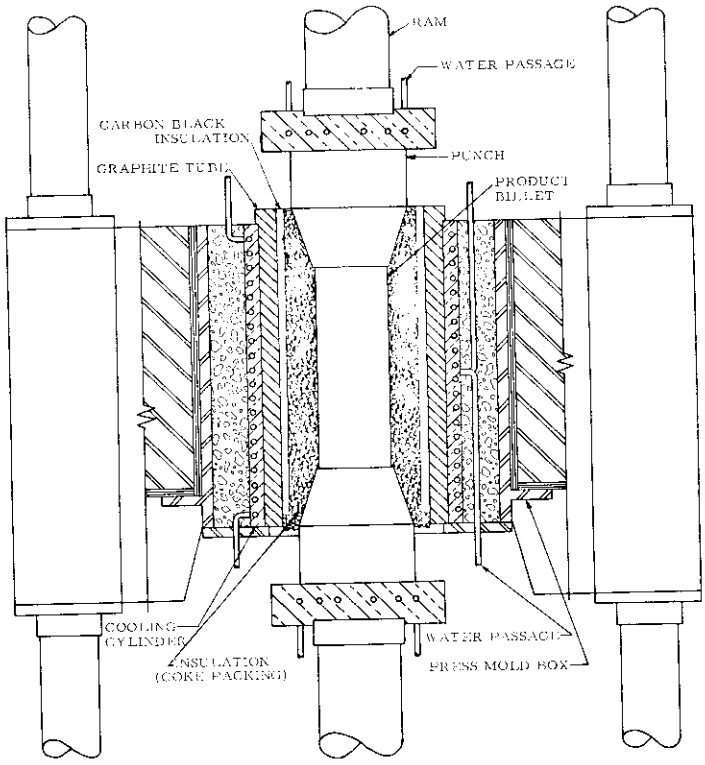

Figure 1. Hot-Pressing Assembly Inserted in Press

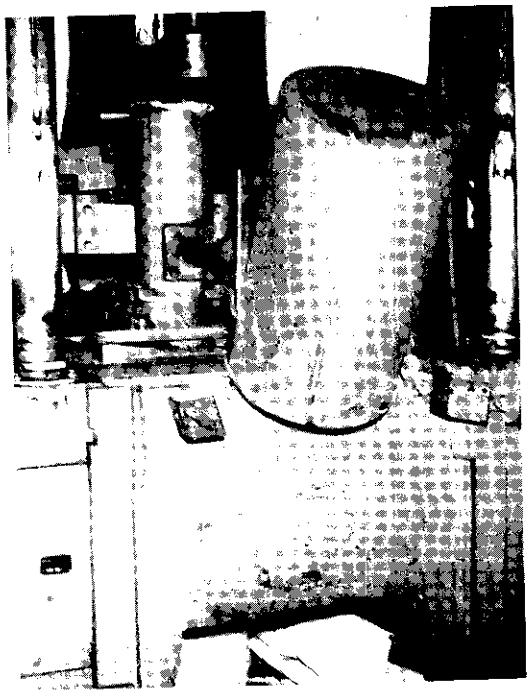

Figure 2. Ejection of ZT Assembly After Hot Pressing

base stocks. Each of these different types of stock will be described as to its properties before and after the hot-pressing process. In the descriptive sections for these different grades, no attempt will be made to completely characterize the material in the hot-pressed form, but rather to find the range into which the material might be placed. In most cases only a few pieces of stock were run, and the property values reported come from a scant number of samples; nevertheless, particular attention is paid to porosimetry. Table 1 lists the units for each property measured.

Table 1. Units of Property Measurements

Properties	Units
Bulk Density*	g/cc
Specific Resistance*	10^{-4} ohm-cm
Young's Modulus*	10^{6} lbs./in.^{2}
Tensile Strength	lbs./in.^{2}
Compressive Strength	lbs./in.^{2}
Flexural Strength*	lbs./in.^{2}
Coefficient of Thermal Expansion (CTE)	10^{-6}/°C (20-100°C)
Thermal Conductivity	cal-cm/sec. cm^2 °K
Admittance	cm^2/sec.
Permeability	Darcys
Porosity	per cent (between 94 and 0.04 microns diameter)
Erosion Rate	mils/sec. (radius)
Photomicrographs	magnification = 100 X

* Each of these is made on the same $\frac{1}{2}$- by $\frac{1}{2}$- by 1-inch sample.

The units used for the above properties hold throughout the report unless otherwise stated, and all tests were made at room temperature. For bulk density, specific resistance, Young's modulus, and flexural strength, a $\frac{1}{2}$- by $\frac{1}{2}$- by 1-inch sample was used. Dimensions were determined with a micrometer to the nearest thousandth of a centimeter and weight to the nearest hundredth of a gram. Bulk density was determined from the dimensional measurements and the weight; specific resistance from measuring the voltage drop in the center section of the sample when in an electrical circuit; Young's modulus by the sonic method; and flexural strength by the third-point loading method. Compressive strength was determined on a 1-inch cube, and tensile strength on a sample with a $1\frac{1}{2}$-inch gauge length which was 0.25 inch in diameter. Room-temperature CTE was determined by comparison with a known sample between room temperature and 100°C. Porosimetry was determined by submerging a small sample in a known volume of mercury and noting the reduction in the volume of mercury as the pressure was increased in increments. This method determined pore sizes from 94 to 0.04 micron in diameter.

Since graphites in general are more or less anisotropic, values for the above properties are usually reported in with- and across-grain directions. Some of the more recently developed graphites and especially the high-density, hot-pressed varieties, exhibit an appreciably increased degree of anisotropy. In many cases, this increased anisotropy is advantageous to the application and permits the graphite to precisely meet the designer's needs. In other cases, the increased anisotropy may be disadvantageous but the other properties make the particular graphite desirable for the given application. For the latter cases, the designer need be aware of the anisotropy and plan accordingly; e.g., the graphite should be used in short lengths or in a stacked washer configuration.

It is again emphasized that the values for graphite properties given in the tables throughout this report are indicative rather than definitive for the experimental ZT materials.

3. HOT PRESSING OF MOLDED GRAPHITE BILLETS

3.1. Grade ZTA Graphite

The previously reported grade ZTA[1] is the archetype of hot-pressed graphites. The properties of ZTA, as well as those of the base stock, or ATJ graphite, from which it is made, are given in Table 2.

Table 2. Physical Properties of Grades ATJ and ZTA Graphite

Property		ATJ Graphite	ZTA Graphite
Bulk Density		1.73	1.94
Specific Resistance	w.g.	11.60	7.00
	a.g.	14.30	22.00
Young's Modulus	w.g.	1.40	2.72
	a.g.	1.15	0.76
Tensile Strength	w.g.	3260	4375
	a.g.	2945	1625
Compressive Strength	w.g.	8330	7100
	a.g.	8530	12400
Flexural Strength	w.g.	4632	5600
	a.g.	4006	2350
CTE	w.g.	2.3×10^{-6}	0.6×10^{-6}
	a.g.	3.5×10^{-6}	9.0×10^{-6}
Thermal Conductivity	w.g.	0.268	0.517
	a.g.	0.215	0.208
Admittance	w.g.	0.3	1×10^{-4}
	a.g.	0.3	3×10^{-4}
Permeability	w.g.	0.020	-
	a.g.	0.015	-

Figure 3 shows porosity for the ATJ graphite and for the finished ZTA. The lines plotted represent cumulative pore volume starting at pore diameters of 94 microns and decreasing to diameters of 0.04 micron. In this range, ZTA has less than half the pore volume of the starting material and does not have a large number of pores of any given size which claim a large share of the volume. Grade ATJ, on the other hand, has a preponderance of pores in the 6- to 8-micron range.

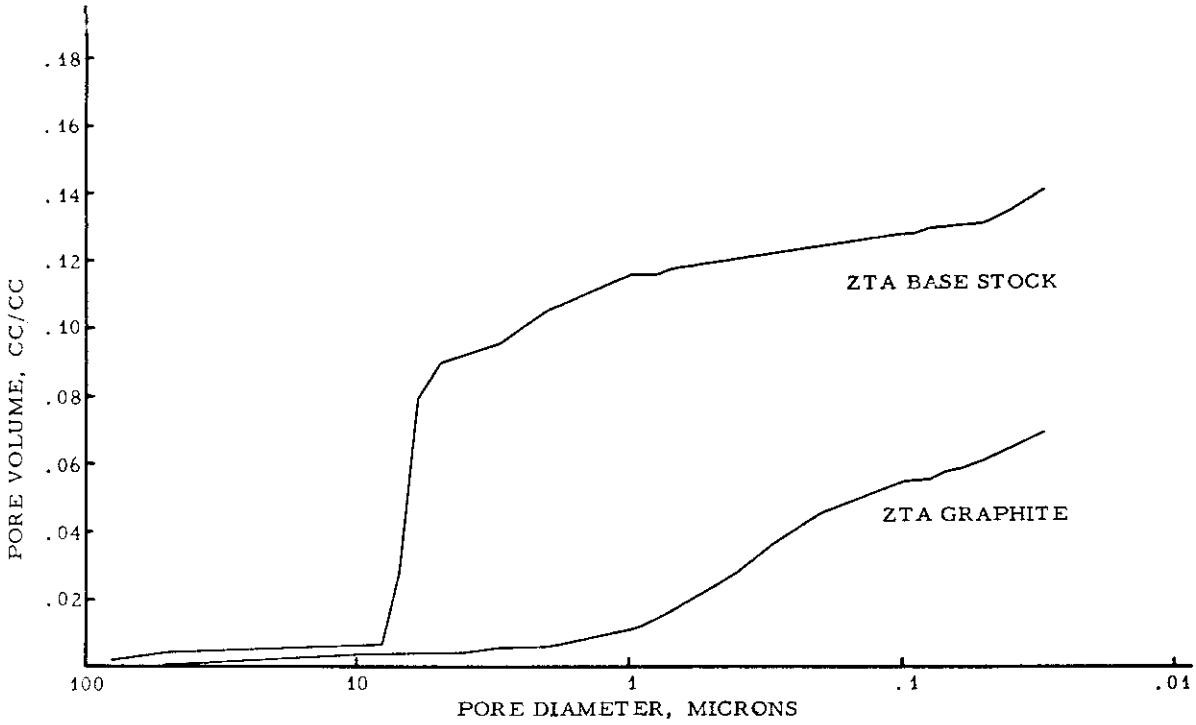

Figure 3. Porosimetry of Grades ATJ and ZTA Graphite

Figures 4 and 5, respectively, are photomicrographs (100 X) of grades ATJ and ZTA. The dark-grey areas in these photographs are pores filled with styrene, and the light-grey areas are graphite. Pores which did not fill with styrene during the mounting process are shown by the black areas. The areas in Figure 4 (before hot pressing) which appear as distinct particles of a relatively dense nature are graphitized coke particles. The connecting material is graphitized binder. Figure 5, the with- and across-grain faces of ZTA, shows the same general configuration, but the pores are smaller with fewer connections between them so that the pores are not filled with styrene during the mounting of the samples for photomicrographic examination. In addition, there appears to be less distinction between particle and binder areas in the ZTA than in the ATJ graphite.

3.2. Investigation of Baking Temperatures

In order to explore the effects of baking temperature on a ZTA-type material, pieces of green stock from which ATJ is made were baked over a temperature range from 900°C to 2800°C. Two pieces were baked at 900°C and two at each temperature ranging from 1400°C to 2800°C in increments of 200°C. Each piece was then hot pressed in the normal manner and measured for physical properties which are given in Table 3. The use of some short statistical methods[2] applied to each property shows that, of the properties listed:

1) There is no correlation between baking temperature and physical properties.

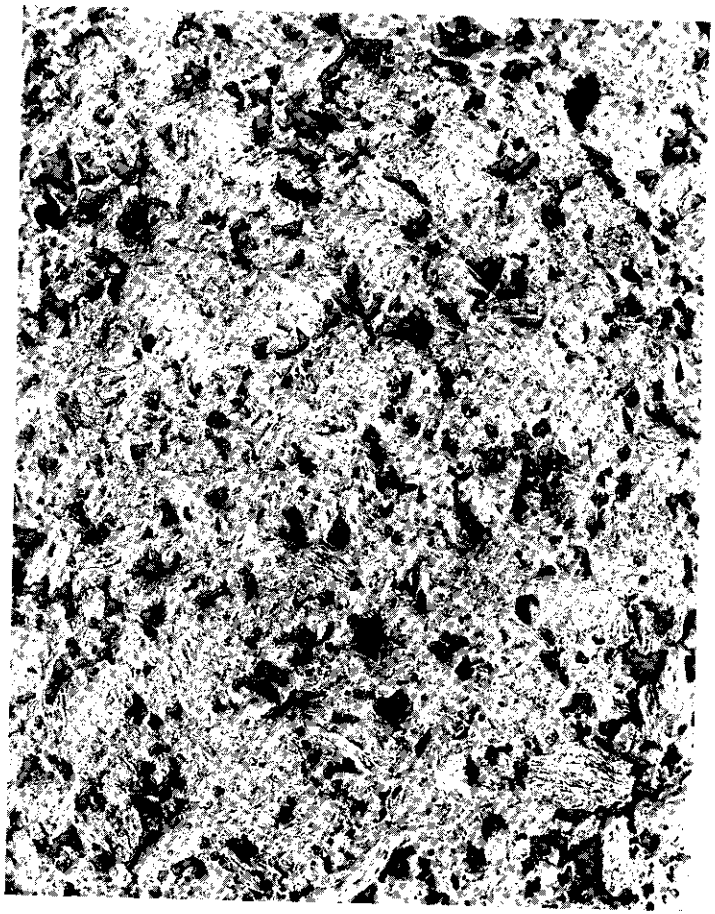

With Grain

Across Grain

Figure 4. Microstructure of Grade ATJ Graphite

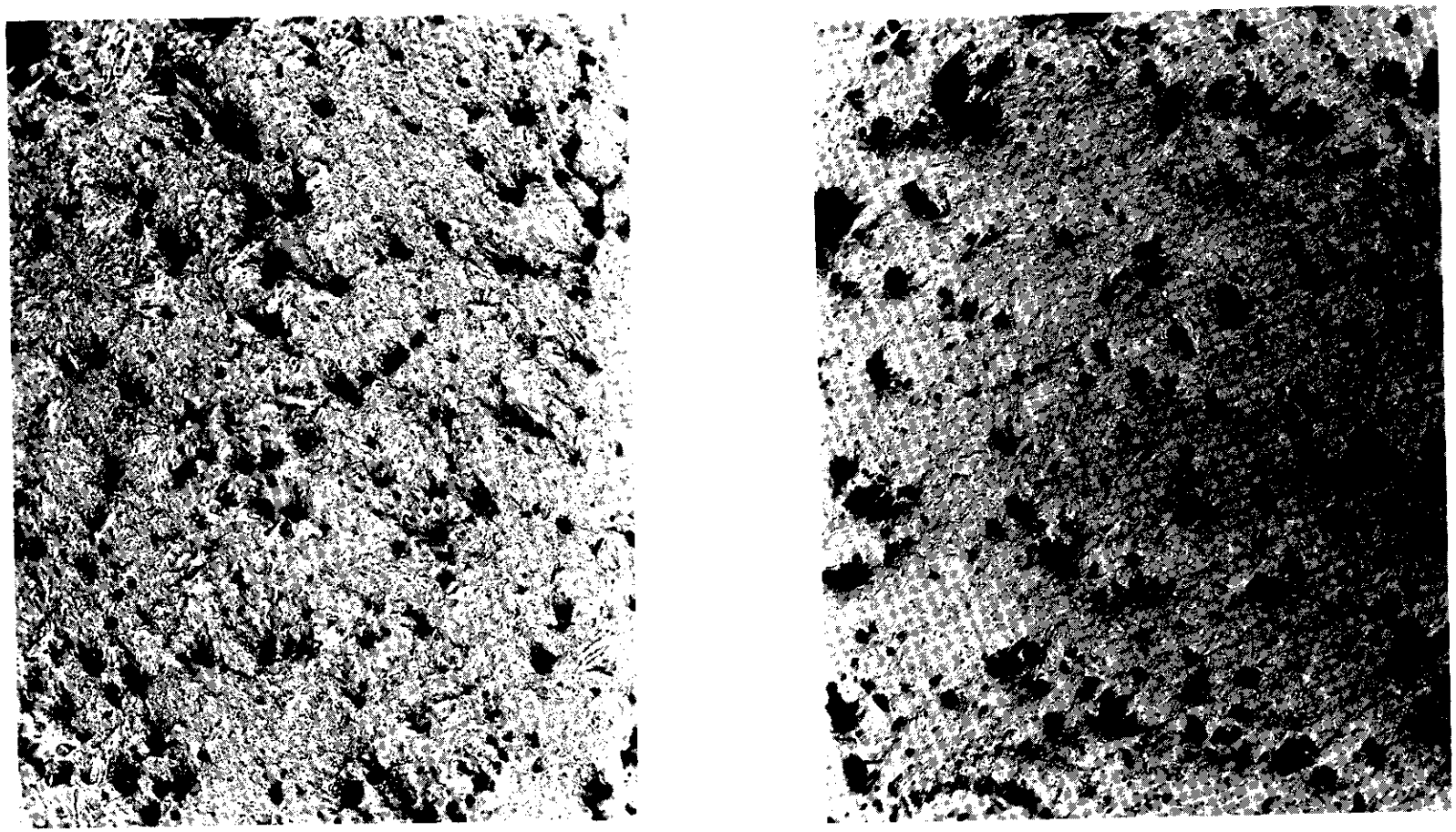

With Grain

Across Grain

Figure 5. Microstructure of Grade ZTA Graphite

2) There is no significant difference among the properties of ZT graphites made from stock baked at different temperatures.

3) All values for each of the properties appear to have a normal distribution.

Comparison of the average values in Table 3 with the values in Table 2 shows that, as a group, hot-pressed graphites made from the material of various baking temperatures behave similarly to grade ZTA. Values of properties for the individual pieces are consistent with the densities observed, with the exception of compressive strength at 1600°C to 1800°C which appears high in the across-grain direction, and at the 2000 °C temperature level where compressive strengths are almost the same in each grain direction. Examination of porosity as shown in Table 3 and in Figures 6 and 7, shows that two distinct groups are formed. Several pieces have total mercury porosity of about $2\frac{1}{2}$ per cent, while most of the others (like ZTA) have porosity of about $6\frac{1}{2}$ per cent. The porosity groups appear independent of baking temperature.

As a check on the first temperature series runs, four more pieces of raw material were baked to 1700°C and four more to 2000°C, and all pieces hot pressed. Physical properties of these latter pieces are shown in Table 4.

Although low density of the 1700°C group hampers comparison, the compressive strength anisotropy ratio for this material is 1.60 to 1 (w.g./a.g.), which compares favorably with ratios between 1.28 and 1.75 to 1 obtained in other lots of ZTA. Except for low across-grain flexural strength, the 2000°C group is the same as grade ZTA.

The porosimetry Figures 6 and 7, when compared with Figure 3, show grade ZTA pore spectra for those pieces each of which has a total porosity of about $6\frac{1}{2}$ per cent. Those pieces each of which has a $2\frac{1}{2}$ per cent total porosity are exceptional. These latter pieces have most of their porosity in the under 0.2-micron diameter range, and the available pores seem fairly evenly distributed as to diameter. A distribution of this type would be expected in material with a density of over 2.00 g/cc but the reason for such distribution in this stock is unknown. Possibly one of the blocks used for the temperature series was of a slightly different variety in the green state and/or reacted differently to impregnating and baking. Efforts to pinpoint the reason for the low porosity were fruitless.

Figures 8 and 9 are photomicrographs, with grain and against grain, of hot-pressed material made from stock baked to 1700°C and 2000°C. Except for differences in lighting intensity and polarization, which affect the clarity of the photographs, the materials appear to be the same and are comparable to grade ZTA.

Table 3. Physical Properties of Hot-Pressed Graphite Versus Baking Temperature of Base Stock

Z No.	Run No.	"Graph" Temp., °C	Bulk Density	Young's Modulus w.g.	Young's Modulus a.g.	Specific Resistance w.g.	Specific Resistance a.g.	Flexural Strength w.g.	Flexural Strength a.g.	Hardness Rockwell "R" ¼" Ball 60 kg w.g.	Hardness Rockwell "R" ¼" Ball 60 kg a.g.	Room-Temp. CTE a.g.	Mercury Porosity, Per Cent	Mercury Bulk Density	Compressive Strength w.g.	Compressive Strength a.g.
21	403	2800	1.939	2.299	.635	715	2189	5514	2158	81	72	8.79	6.9	1.947	2760	13,875
22	404	2800	1.931	2.734	.632	581	2105	5774	2120	77	75	8.94	2.2	1.940	5480	11,219
23	405	2600	1.926	2.313	.631	698	2152	4913	2040	77	74	8.94	6.1	1.950	4440	10,646
25	407	2400	1.938	2.820	.691	704	2006	6056	2481	81	87	8.71	2.7	1.947	7882	12,642
26	408	2400	1.958	2.499	.685	727	1987	5805	2426	84	80	8.84	6.1	1.951	8125	10,934
27	409	2200	1.939	2.433	.765	720	1872	5987	2736	86	83	8.61	5.7	1.942	7866	8,520
28	410	2200	1.967	3.147	.677	597	2320	6612	2256	88	82	10.21	3.1	1.942	7738	8,669
29	411	2000	1.905	2.606	.729	597	1738	6063	2638	79	79	8.09	6.1	1.830	8589	8,982
30	412	2000	1.985	3.092	.687	646	2395	7181	2100	90	88	9.85	2.7	1.975	8535	8,471
31	413	1800	1.956	2.804	.693	810	2418	6435	2233	88	84	9.61	0.5*	1.826	8310	13,399
32	414	1800	1.922	2.697	.663	684	2246	5937	2162	83	79	9.61	6.8	1.934	7422	13,520
33	415	1600	1.983	3.177	.706	642	2305	7276	2351	92	88	10.15	2.5	1.973	8320	14,481
34	416	1600	1.940	2.341	.675	738	2145	5757	2240	83	80	9.45	6.6	1.946	7234	12,625
35	417	1400	1.951	2.775	.765	675	2021	5898	2165	108	106	9.12	6.8	1.905	8275	8,634
36	418	1400	1.927	2.704	.514	709	2523	5261	1843	107	102	9.92	9.8	1.844	6586	8,110
37	419	900	1.936	2.666	.730	716	2137	6651	2157	109	104	9.36	5.5	1.953	8334	8,539
38	420	900	1.948	2.716	.712	692	2143	6113	1900	106	107	9.25	3.9	1.953	8168	8,490
Avg.		-	1.944	2.695	.682	685	2159	6073	2236	89	87	9.26	4.9	1.927	7298	10,692

*Probably Wrong

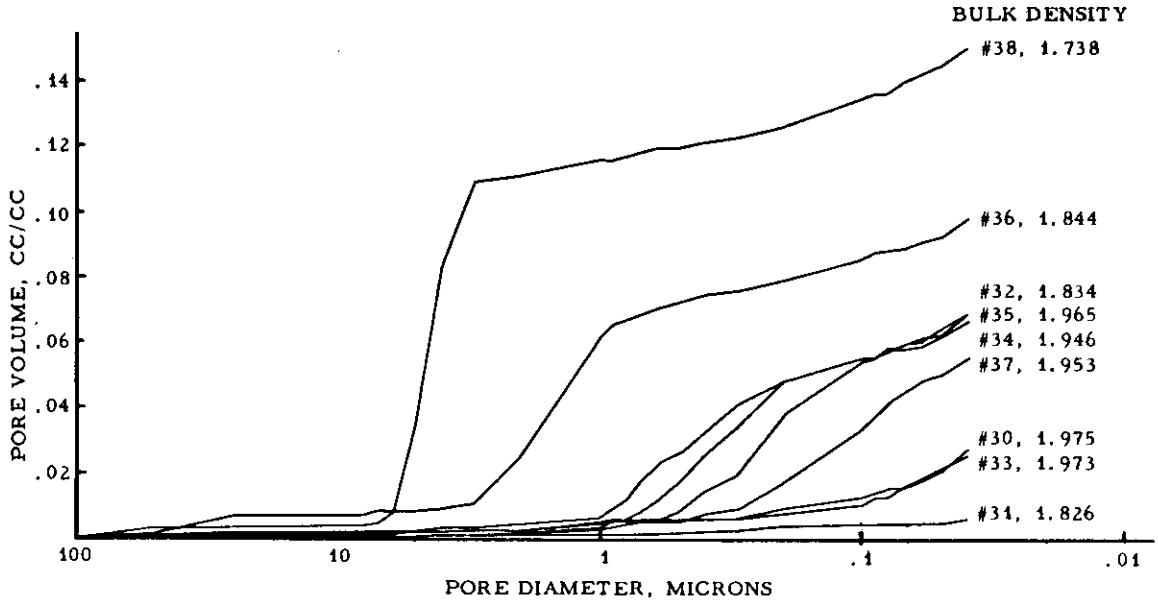

Figure 6. Porosimetry of Hot-Pressed Graphite Made from Material of Various Baking Temperatures, ZT Nos. 30 through 36

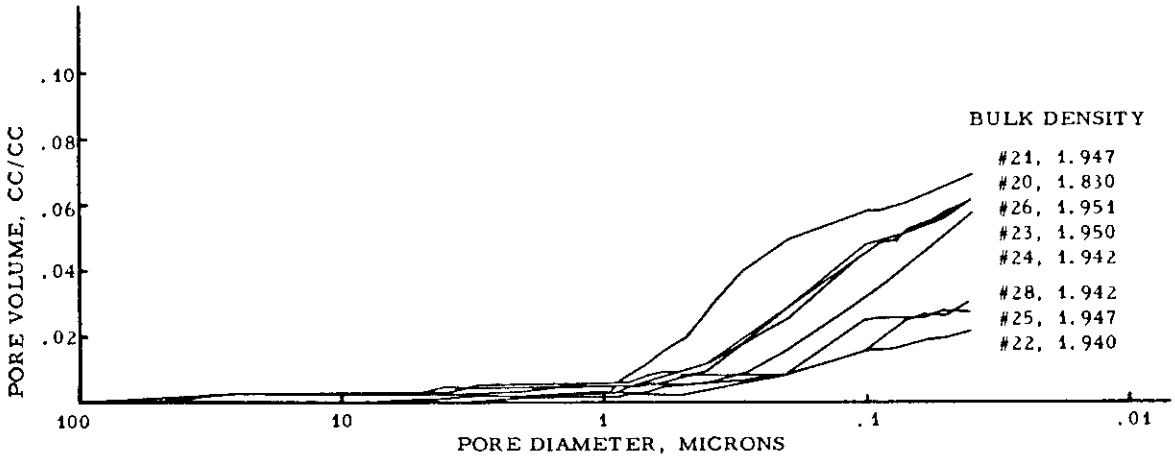

Figure 7. Porosimetry of Hot-Pressed Graphite Made from Material of Various Baking Temperatures, ZT Nos. 21 through 26, 28 and 29.

Table 4. Physical Properties of Hot-Pressed Graphite from Stock Baked to 1700°C and 2000°C

Property		1700°C	2000°C
Bulk Density		1.915	1.954
Young's Modulus	w.g.	2.158	2.527
	a.g.	.618	.620
Specific Resistance	w.g.	7.07	6.25
	a.g.	20.11	20.82
Flexural Strength	w.g.	4681	4731
	a.g.	1694	1350
Compressive Strength	w.g.	6265	5945
	a.g.	9999	10533
CTE	a.g.	7.79	
Rockwell Hardness "R"	w.g.	96.3	
	a.g.	98.5	
Mercury Porosity		7.23	

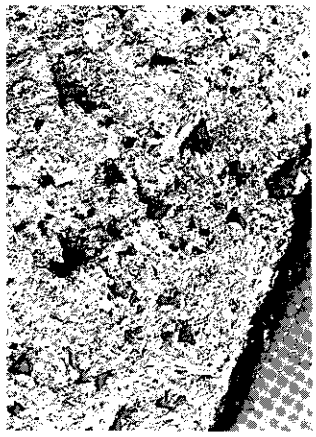

With Grain

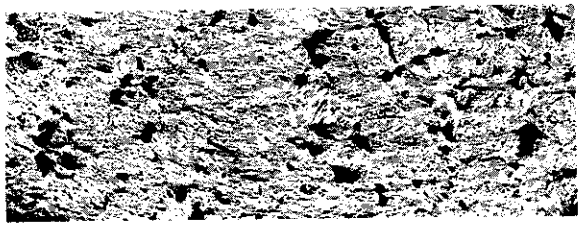

Across Grain

Figure 8. Microstructure of Hot-Pressed Graphite from Stock Baked to 1700°C

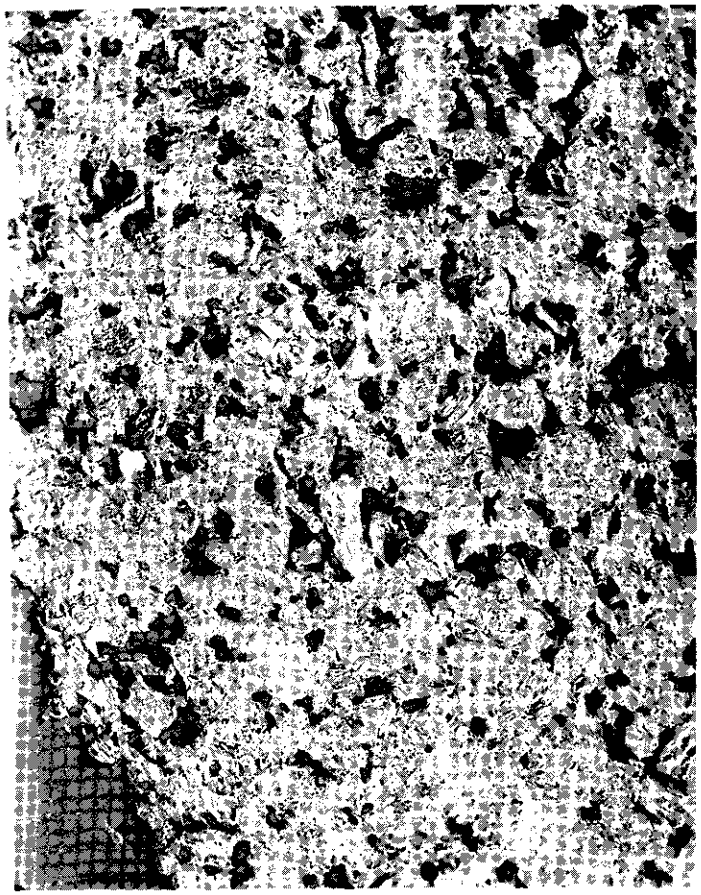

With Grain

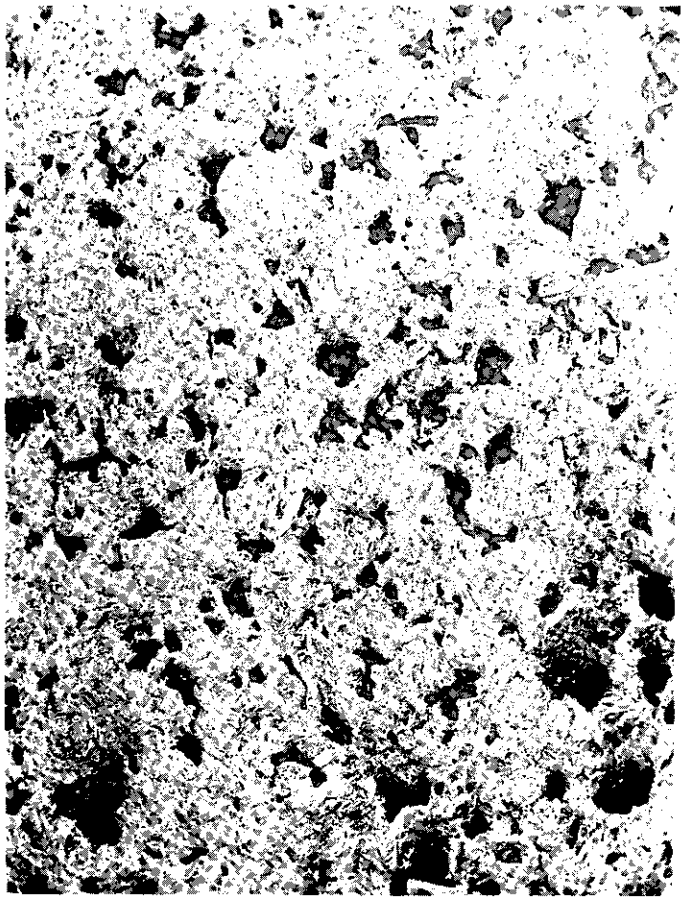

Across Grain

Figure 9. Microstructure of Hot-Pressed Graphite from Stock Baked to 2000°C

It was concluded from the trials of baking temperature that no significant improvement over ZTA would be forthcoming by changing the final processing temperature before hot pressing. It is possible, however, due to the time and handling involved, that one temperature would offer economic advantages over the others.

3.3. Grade ZTB Graphite

Grade ZTB graphite, like ZTA, is made using ATJ as the base material. By using more severe hot pressing conditions, the ZTB graphite attains a higher density (1.97 to 2.02 g/cc) than does the ZTA graphite (1.92 to 1.97 g/cc). In addition, grade ZTB exhibits a higher degree of anisotropy and a lower porosity than grade ZTA.

Another method of increasing the density and decreasing the porosity of a ZT graphite is by impregnation[3] of the base stock before hot pressing. This method was used with ATJ graphite and, in most cases, one impregnation was sufficient to produce hot-pressed graphites with densities greater than 1.98 g/cc (grade ZTB). Porosity of the stock was reduced to about 3 per cent, or less than half that of grade ZTA. The denser, less porous material made from impregnated ATJ does not differ significantly, as shown by physical property measurements, from ZTB graphite made directly from ATJ graphite by more severe hot pressing. The properties of the ZTB graphite fabricated from the impregnated ATJ are shown in Table 5.

Table 5. Physical Properties of Grade ZTB Graphite Fabricated from Impregnated ATJ Graphite

Property		Value
Bulk Density		2.01
Specific Resistance	w.g.	6.60
	a.g.	21.62
Young's Modulus	w.g.	3.57
	a.g.	0.77
Tensile Strength	w.g.	5383
	a.g.	-
Compressive Strength	w.g.	9110
	a.g.	13080
Flexural Strength	w.g.	6230
	a.g.	2470
CTE	w.g.	0.5
	a.g.	9.8
Thermal Conductivity	w.g.	0.465
	a.g.	0.177
Admittance	w.g.	1×10^{-4}
	a.g.	2×10^{-4}

Grade ZTB is a more highly oriented material than ZTA. Comparison of the properties in Table 5 with those in Table 2 shows a CTE anisotropy ratio of about 40 to 1 for ZTB, while the same ratio for ZTA is 15 to 1. ZTB, because of its greater degree of crystal alignment, has greater tensile and flexural strengths in the with-grain directions than ZTA and lower strengths in the across-grain direction. Specific resistance, compressive strength, and CTE are less in the with-grain direction, and greater in the across-grain direction for ZTB than for ZTA. Total mercury porosity (Figure 10) of the ZTB is less than half that of ZTA. Less than one-third of the porosity of ZTB lies in pores with diameters greater than 1.0 micron, while half of its porosity is in pores below 0.1 micron in diameter. Between 1 and .04 micron the curve is much smoother for ZTB than for ZTA, showing no one particular pore diameter having a large part of the pore volume.

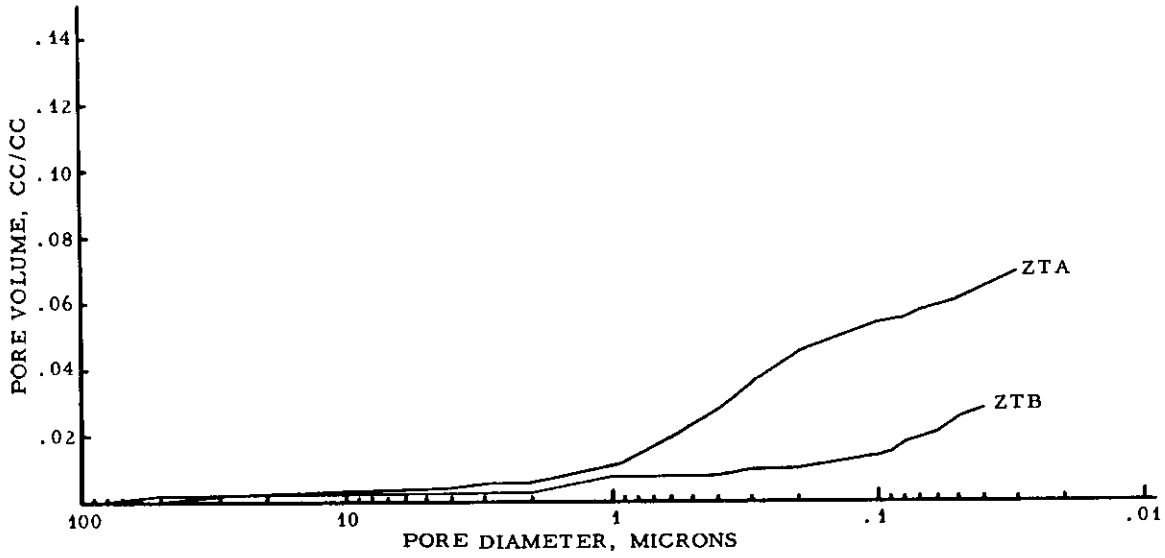

Figure 10. Porosimetry of Grades ZTA and ZTB Graphite

The differences in the microstructure of ZTB and ZTA can be seen by comparing Figure 11 with Figure 5. Figure 5 shows ZTA with- and across-grain photomicrographs in which a number of large pores are visible, and individual grains are not completely ordered. Grade ZTB has fewer large pores, and the individual grains are more oriented than for grade ZTA. The grain orientation is more evident in the with-grain photographs.

It was concluded from this work that the most practical way to obtain high density and low porosity for ZT graphite was to impregnate the base stock before hot working. The designer who considers using this material must remember that a greater degree of anisotropy exists for ZTB than for ZTA.

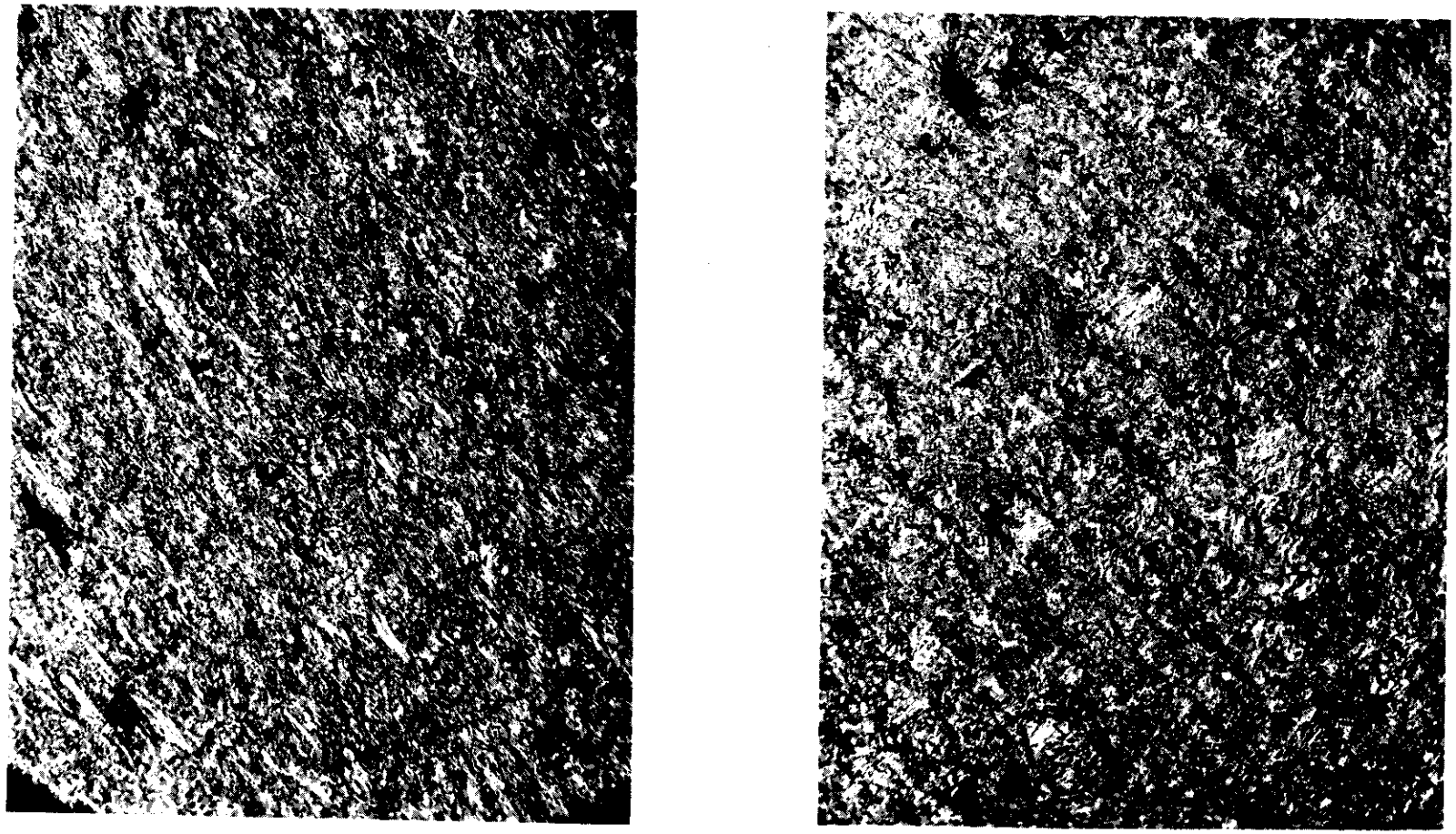

With Grain

Across Grain

Figure 11. Microstructure of Grade ZTB Graphite

3.4. Hot Pressing of Grade CFW Graphite

Grade CFW, impregnated grade ATL, was investigated as a base stock to produce ZT graphite with a low CTE anisotropy ratio. Grade CFW has a larger grain size and a lower CTE anisotropy ratio than the raw material for ZTA. An impregnation step is used in the processing of CFW in order to increase density and to impart extra strength to the material. Density of the material is about 1.88 g/cc. The total porosity of CFW is about 6 per cent, which places it in the range of ZTA, but Figure 13 shows that the shape of the porosity curve is different from that of ZTA given in Figure 10. CFW has much more of its porosity in larger diameter holes than does ZTA. More than half the total porosity of the CFW lies above 1.0 micron. The photomicrographs in Figure 12 show the much larger grain size of the CFW than that of the graphite used for grade ZTA. In the center of the with-grain photomicrograph, one large grain takes up about 20 per cent of the area of the picture. Especially noticeable in the across-grain photomicrograph is the effect of impregnation. The impregnant, which shows up as light-colored areas centered in the darker pores, is of a nongraphitizing type and appears to have no structural order on rebaking. A summary of CFW properties is given in Table 6.

Table 6. Physical Properties of Grade CFW Graphite

Property		Value
Bulk Density		1.89
Specific Resistance	w.g.	11.79
	a.g.	12.48
Young's Modulus	w.g.	1.54
	a.g.	1.41
Tensile Strength	w.g.	1950
	a.g.	1760
Compressive Strength	w.g.	7350
	a.g.	7730
Flexural Strength	w.g.	2470
	a.g.	2460
CTE	w.g.	2.5
	a.g.	2.8
Thermal Conductivity	w.g.	0.310
	a.g.	0.295
Admittance	w.g.	1.4×10^{-2}
	a.g.	0.9×10^{-2}
Permeability	w.g.	0.003
	a.g.	0.004
Mercury Porosity		9.1

With Grain

Across Grain

Figure 12. Microstructure of Grade CFW Graphite

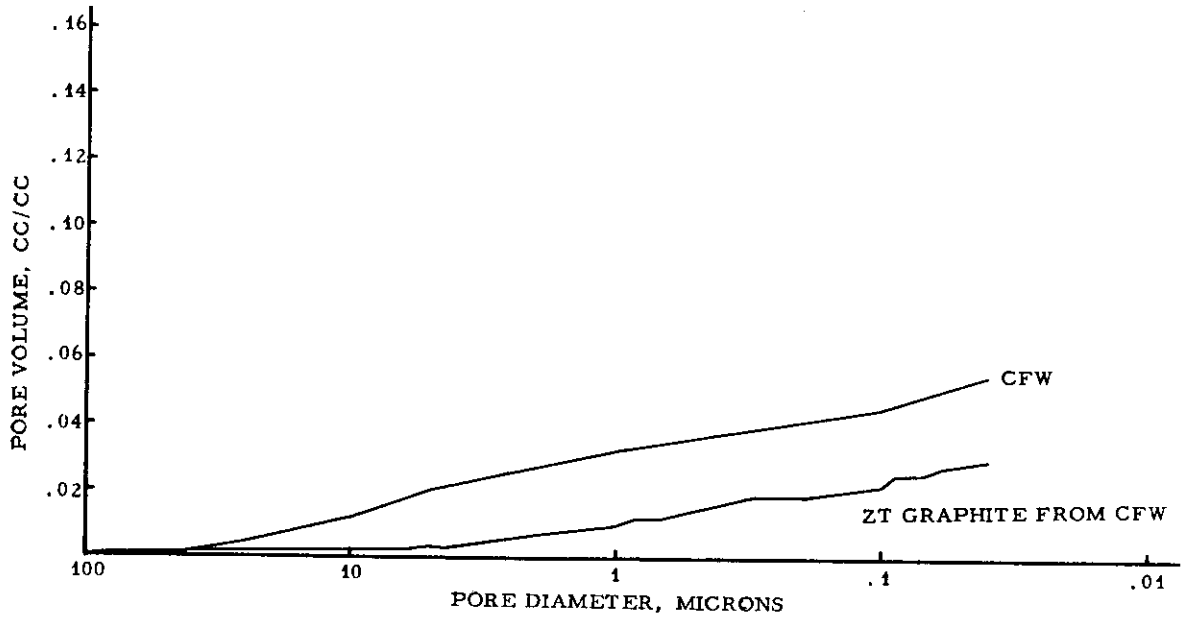

Figure 13. Porosimetry of Grades CFW and CFW/ZT Graphite

The original piece of ZT graphite made from CFW was used for a rocket nozzle test rather than for physical property measurements. It was expected that the erosion rate for this material would be between 0.1 and 0.3 mils/sec. on the radius, but the actual erosion rate was 0.9 mils/sec. and, consequently, the decision was made to discontinue hot-pressing trials with grade CFW graphite. Specimens from this one piece were used to run porosimetry tests, the results of which are plotted in Figure 13, along with the CFW before hot pressing. It appears that hot pressing has reduced porosity over the entire range for the material, but especially in the range between 1 and 50 microns. Density of the CFW was raised by hot pressing to 1.962 g/cc at the most dense portion measured.

3.5. Multidirection Hot-Working Trials

Attempts were made to apply the hot-pressing process in one grain direction, turn the piece 90°, and hot press in the other grain direction in an effort to reduce the anisotropy of hot-worked graphite. It was hoped that by this means a material of very high density and low porosity could be produced with a minimum of crystal alignment. The material chosen for these trials was grade ATL, a molded graphite having a maximum grain size of 0.03 inch. Some of this material was hot pressed in large sizes, and then impregnated to further increase its density. Figures 14 and 15 show the material after the first hot-pressing process. Figure 14 shows a portion of the material which had a bulk density of 1.7 g/cc, while the material in Figure 15 had a density of 1.9 g/cc. Four pieces of this hot-pressed stock were machined and hot pressed a second time with the direction of pressure being at right angles to the direction of the original hot pressing pressure. In each case, the stock shattered shortly after heating was begun, presumably because of thermal shock. Even with careful application of pressure at a slow heating rate,

the stock appeared as in Figure 16. Whether or not the desired result could be obtained by modification of the hot-working process still has not been resolved.

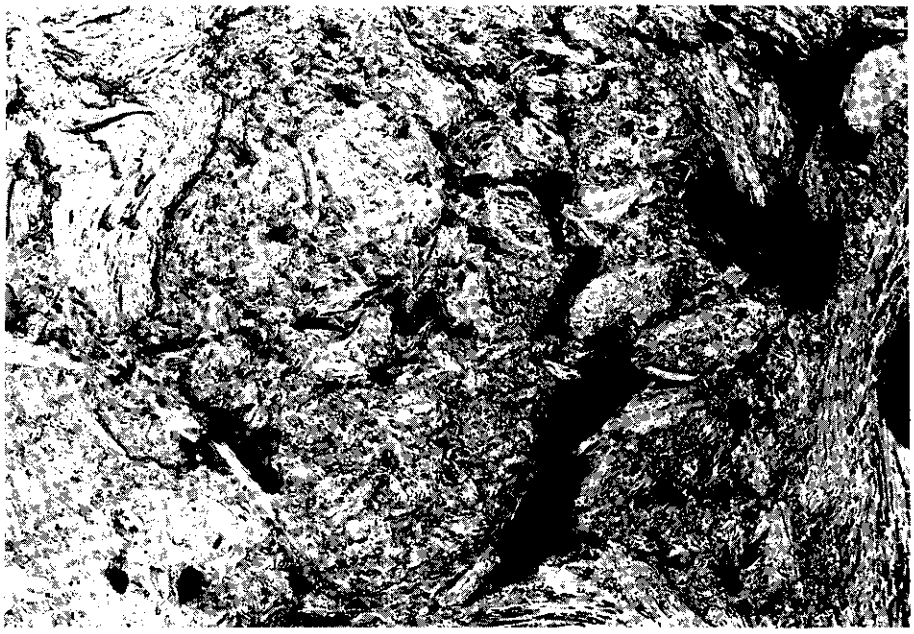

Figure 14. Microstructure of Grade ATL/ZT Graphite, 1.7 g/cc Bulk Density

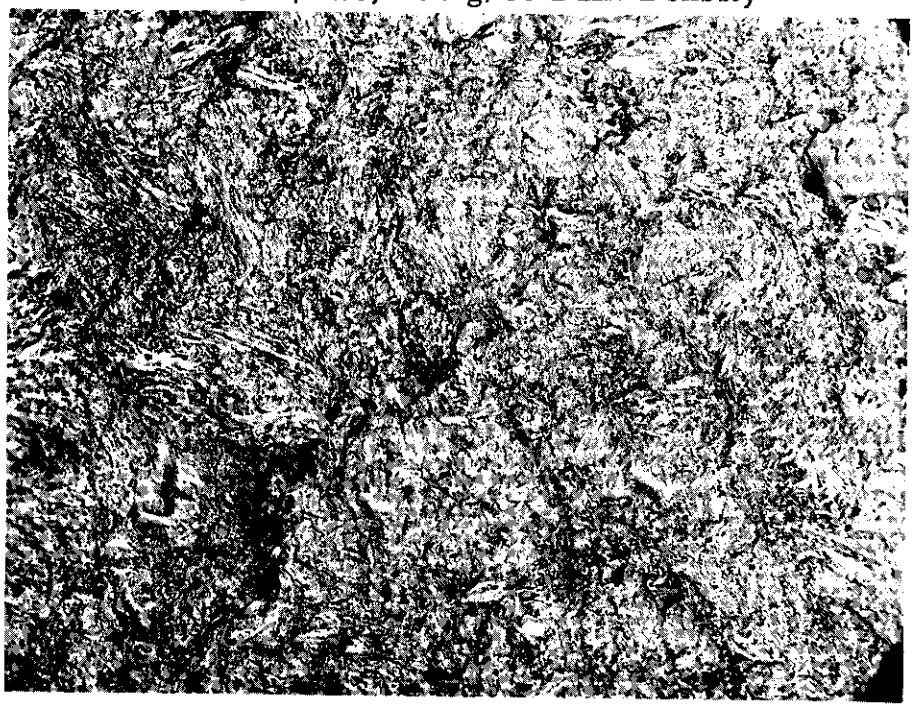

Figure 15. Microstructure of Grade ATL/ZT Graphite, 1.9 g/cc Bulk Density

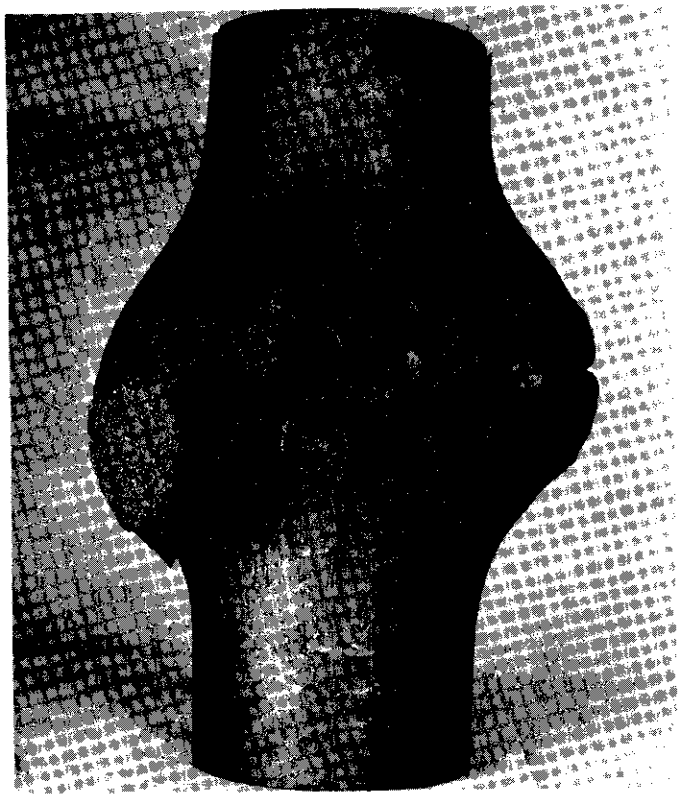

Figure 16. Result of Multidirection Hot-Working Trial

3.6. Hot Pressing of Resin-Bonded Graphite

In developing new graphite materials, particularly for aerospace applications, one method of changing graphite properties was to use a new binder system.[4] In one system prepolymerized furfural alcohol-paratoluene sulfonic acid was used as a replacement for pitch binder. Several blocks were made using this resin binder system and two of the blocks were used for hot-pressing trials. After hot pressing the material to a length reduction of 25 per cent, it was found to have some internal cracks, but enough good material was available to measure a few physical properties (see Table 7).

Table 7. Physical Properties of Resin-Bonded Graphite Before and After Hot Pressing

Property		Before Hot Pressing	After Hot Pressing
Bulk Density		1.62	1.949
Specific Resistance	w.g.	9.8	7.40
	a.g.	14.0	
Young's Modulus	w.g.	1.08	
	a.g.	0.67	
Flexural Strength	w.g.	2240	3739
	a.g.	1710	

Figure 17 shows porosimetry curves for the material both before and after hot pressing. Although the total porosity of the stock was high (approximately 24 per cent), the porosity was reduced by hot pressing to less than 5 per cent, or slightly below the ZTA range. Figure 18 is a photomicrograph of the hot-pressed material. This photograph indicates a material not unlike ZTB in pore structure, with few large pores evident, but there does not appear to be as great a degree of grain orientation as in ZTB.

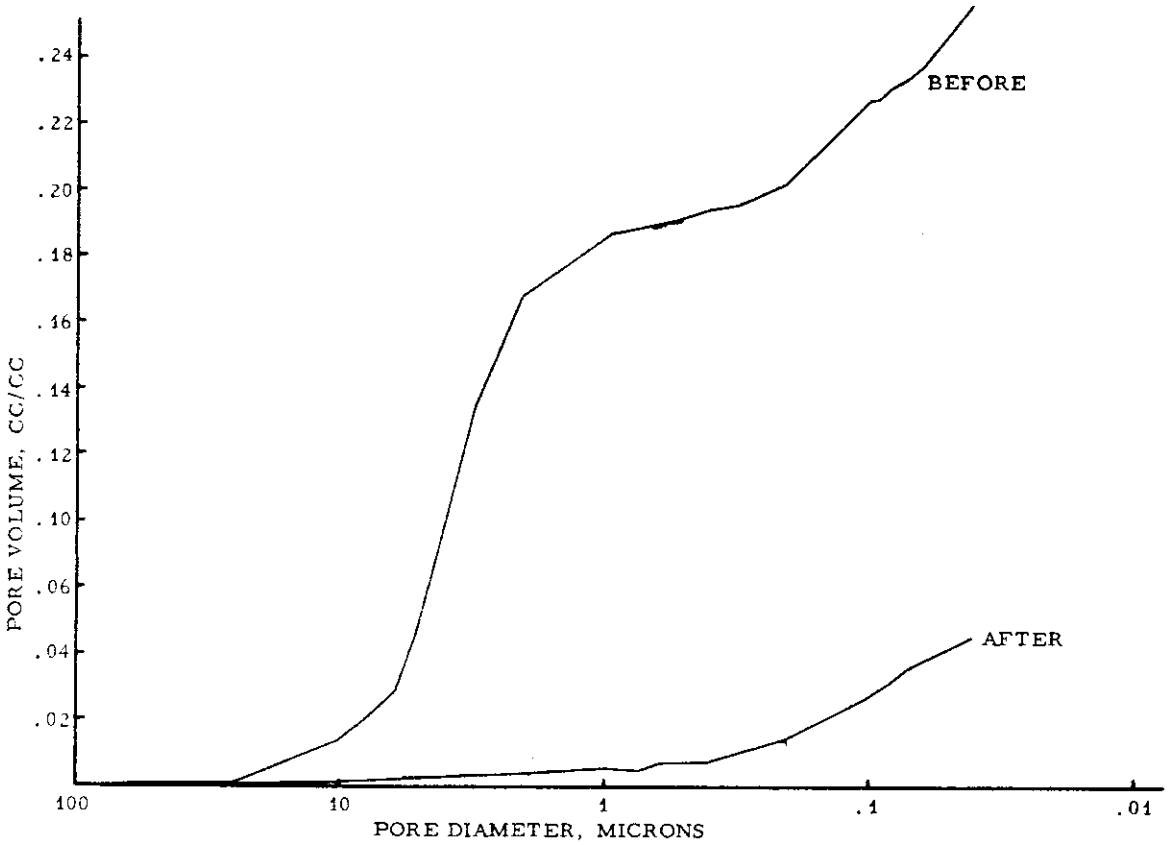

Figure 17. Porosimetry of Resin-Bonded Graphite Before and After Hot Pressing

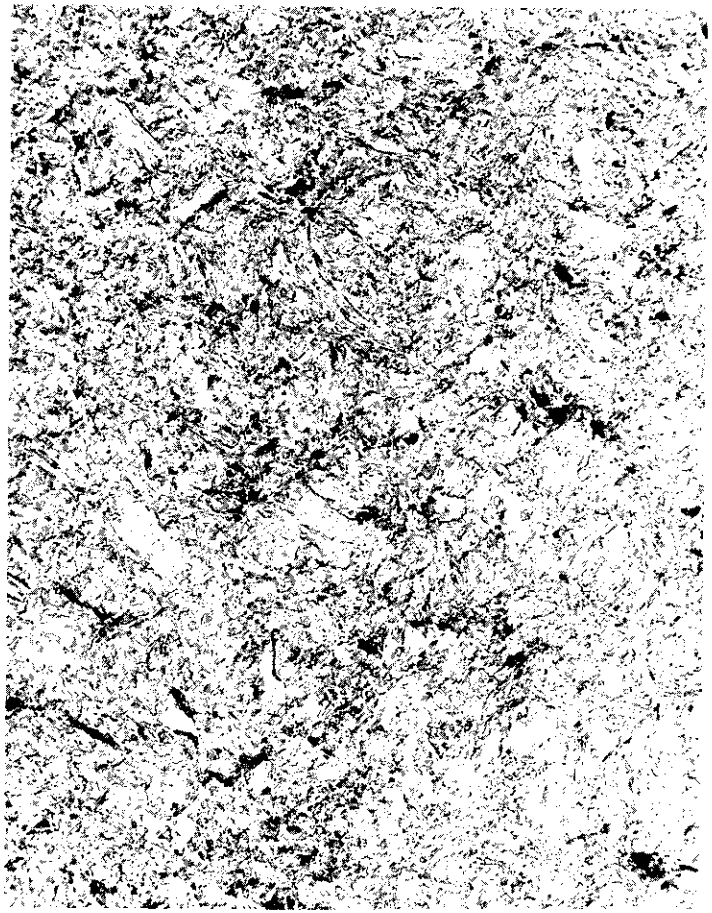

With Grain

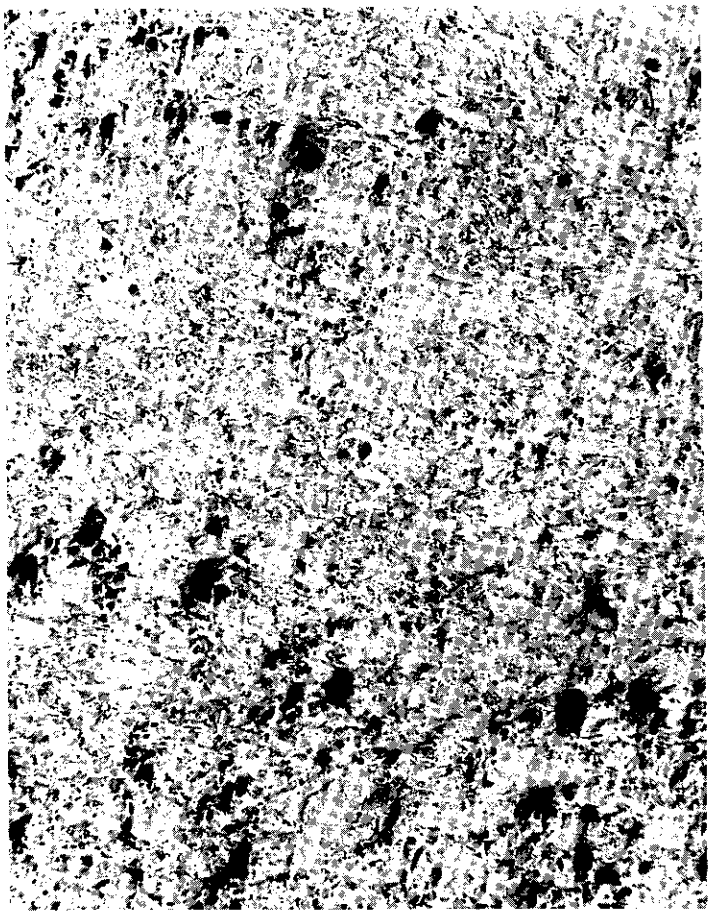

Across Grain

Figure 18. Microstructure of ZT Graphite from Resin-Bonded Stock

4. HOT PRESSING OF PRESSURE-CURED GRAPHITES

4.1. Grades ZTE and ZTF Graphite

In scaling up ZT products to large diameters[5] it was found that the most suitable fine-grain base stock for grade ZTE is a pressure-cured graphite (grade RVA[6]) with a bulk density of about 1.85 g/cc and a total mercury porosity of about 10 per cent, which are respectively higher and lower than for ATJ graphite used as the base material for grade ZTA. Figure 19 shows the porosimetry of the grade RVA material used as a base stock for ZTE. The curve is similar to that for grade ATJ; however, there is not quite as sharp a vertical break in the 8- to 10-micron range showing that the RVA has fewer pores 8 to 10 microns in diameter. Comparing the photomicrograph of RVA (Figure 20) with the photomicrograph of ATJ (Figure 4) shows that the former has a larger grain size. Further comparison, especially in the with-grain direction, emphasizes the difference in pore structure of the two materials.

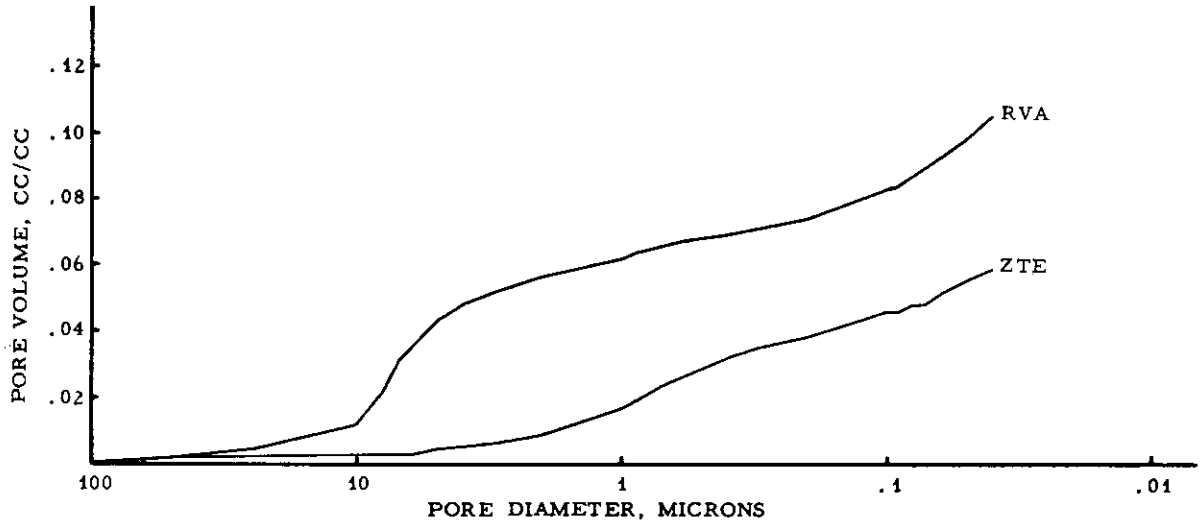

Figure 19. Porosimetry of Grades ZTE and RVA Graphite

The physical properties of grade RVA, the base material for ZTE, given in Table 8 show that the pressure-cured graphite has a slightly lower strength and CTE anisotropy ratio than does grade ATJ used for ZTA graphite fabrication. Density is the major difference between the two materials. Because of the high density of pressure-cured stock, it was hoped that less vigorous hot pressing would produce material with density and porosity similar to ZTA, but with less grain orientation. This aim was accomplished with a length reduction of under 10 per cent.

Crystal alignment of the ZTE is less than that of ZTA as exemplified by the ratio of with-grain and across-grain CTE's. For ZTA the with-grain CTE is 15 times greater than the across-grain value, while for ZTE this ratio has been reduced to less than 8 to 1. The porosimetry curve for ZTE shows a porosity very similar to ZTA; total pore volume,

and the distribution of the various pore sizes, is much the same for the two materials. As with ZTA, the porosity of ZTE is half that of its base stock. Figure 21, photomicrographs of ZTE in both grain directions, gives a good indication of how the pores are collapsed and the individual grains are squeezed together during hot pressing. The ordering of the grain structure is more evident in the with-grain photomicrograph. Comparison of Figures 20 and 21 shows the particles to be more randomly distributed in the base material than in the ZTE. The black spots in the latter picture are areas of the sample which were not fully impregnated with styrene during the sample preparation.

Table 8. Physical Properties of Grades ZTE and RVA Graphite

Property		RVA Graphite	ZTE Graphite
Bulk Density		1.84	1.96
Specific Resistance	w.g.	12.13	8.95
	a.g.	15.62	20.40
Young's Modulus	w.g.	1.78	2.44
	a.g.	1.28	0.80
Tensile Strength	w.g.	2995	3210
	a.g.	2170	1470
Compressive Strength	w.g.	9325	5760
	a.g.	8750	6780
Flexural Strength	w.g.	3735	4335
	a.g.	2950	2315
CTE	w.g.	1.7	0.8
	a.g.	2.8	6.8
Thermal Conductivity	w.g.	0.280	0.352
	a.g.	0.238	0.194
Admittance	w.g.	2×10^{-2}	2×10^{-3}
	a.g.	2×10^{-2}	4×10^{-3}

In selecting a material with a maximum grain size of 0.03 inch as the base material for ZTE, it was expected that some sacrifice in strengths would have to be made. Compressive strength of ZTE in the across-grain direction is about half that of ZTA, although the with-grain strengths of the two materials differ by less than 20 per cent.

Hot pressing of the pressure-cured stock at higher pressures and temperatures produced a material with a bulk density of about 2.0 g/cc. The physical properties of this graphite, designated as grade ZTF,

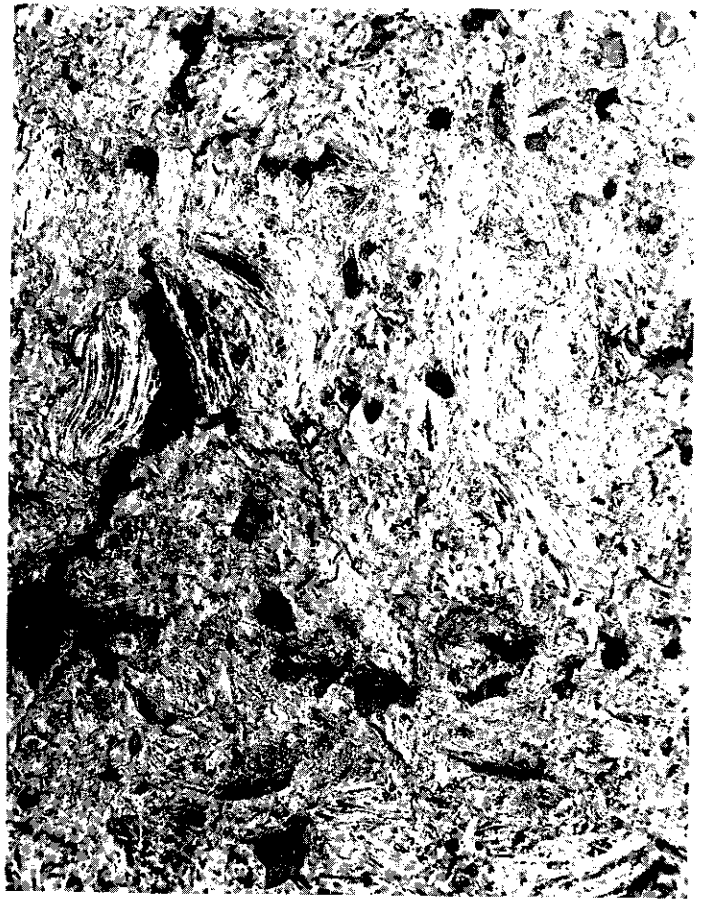

With Grain

Across Grain

Figure 20. Microstructure of Grade RVA Graphite

With Grain

Across Grain

Figure 21. Microstructure of Grade ZTE Graphite

are given in Table 9. Anisotropy of ZTF, with a CTE ratio of less than 12 to 1, is midway between ZTA and ZTE. Compressive strength for ZTF is higher in both grain directions than for ZTE, the weaker direction being within 2000 lbs./in.^{2} of ZTA. Porosimetry, as shown in Figure 22, parallels that of ZTE, but the ZTF has about 40 per cent less total pore volume.

Table 9. Physical Properties of Grade ZTF Graphite

Property		Value
Bulk Density		2.00
Specific Resistance	w.g.	7.40
	a.g.	20.06
Young's Modulus	w.g.	2.76
	a.g.	0.76
Compressive Strength	w.g.	6930
	a.g.	8940
Flexural Strength	w.g.	3875
	a.g.	1505
CTE	w.g.	0.6
	a.g.	8.0
Thermal Conductivity	w.g.	0.374
	a.g.	0.081
Admittance	w.g.	2×10^{-4}
	a.g.	7×10^{-5}

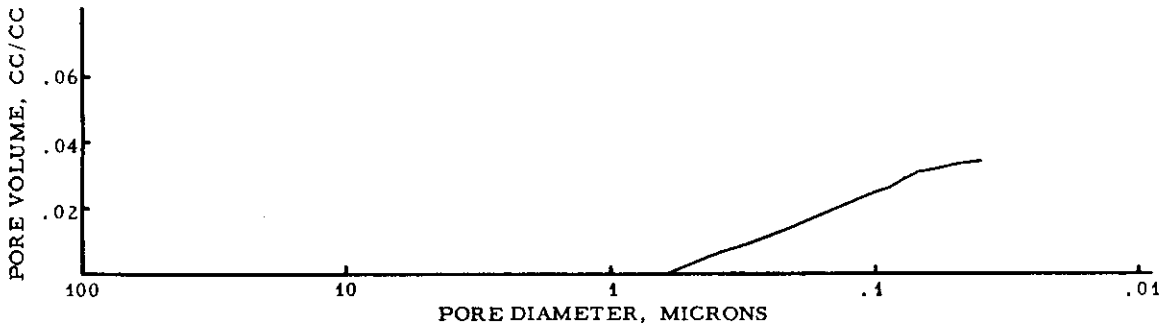

Figure 22. Porosimetry of Grade ZTF Graphite

Photomicrographs (Figure 23) again show the collapsing of the pores which is especially evident in the across-grain photograph.

4.2. Hot Pressing of Grade CFZ Graphite

Grade CFZ is obtained by impregnating RVA graphite. The impregnation results in an increased density (1.91 g/cc or higher), reduced porosity (below 5 per cent), and increased strengths. Figure 24 shows the with-grain and across-grain structure of CFZ. Both of these photomicrographs show the mixture of large and small grains typical of this material. The ungraphitized impregnant can be seen as the light areas surrounded by black. Other physical properties of CFZ are in Table 10. The porosity curve for CFZ (Figure 25) showing a large portion of the pore volume existing in pores of 0.5 to 3.0 microns in diameter is not unlike that for ZTA.

With these characteristics, it was hoped that the stock could be given a minimum of hot pressing while attempting to obtain high density and low porosity, and still have low anisotropy ratios. Densification of CFZ by hot pressing, however, was found to be extremely difficult. All but one of the attempts to make ZT material from CFZ stock were unsuccessful. In the one successful trial, the density was increased to 1.94 g/cc with a length reduction of less than 20 per cent. The total porosity, shown in Figure 25, was approximately 6 per cent. The volume of pores with diameters between 1.0 and 3.0 microns was decreased considerably from that in the original CFZ. Physical properties obtained from the one piece of hot-pressed CFZ are shown in Table 10.

Table 10. Physical Properties of Grade CFZ Graphite Before and After Hot Pressing

Property		CFZ	CFZ/ZT	
Bulk Density		1.90	1.94	1.92
Specific Resistance	w.g.	12.03	7.17	7.83
	a.g.	14.44	26.27	37.8
Young's Modulus	w.g.	1.88	2.564	1.836
	a.g.	1.52	0.513	0.338
Tensile Strength	w.g.	3840		
	a.g.	2490		
Compressive Strength	w.g.	10195		3016
	a.g.	11365		1491
Flexural Strength	w.g.	3895	3431	1021
	a.g.	3280	1857	355
CTE	w.g.	2.0		
	a.g.	2.5		
Thermal Conductivity	w.g.	0.316		
	a.g.	0.280		
Admittance	w.g.	3×10^{-4}		
	a.g.	3×10^{-4}		
Mercury Porosity			5.7	

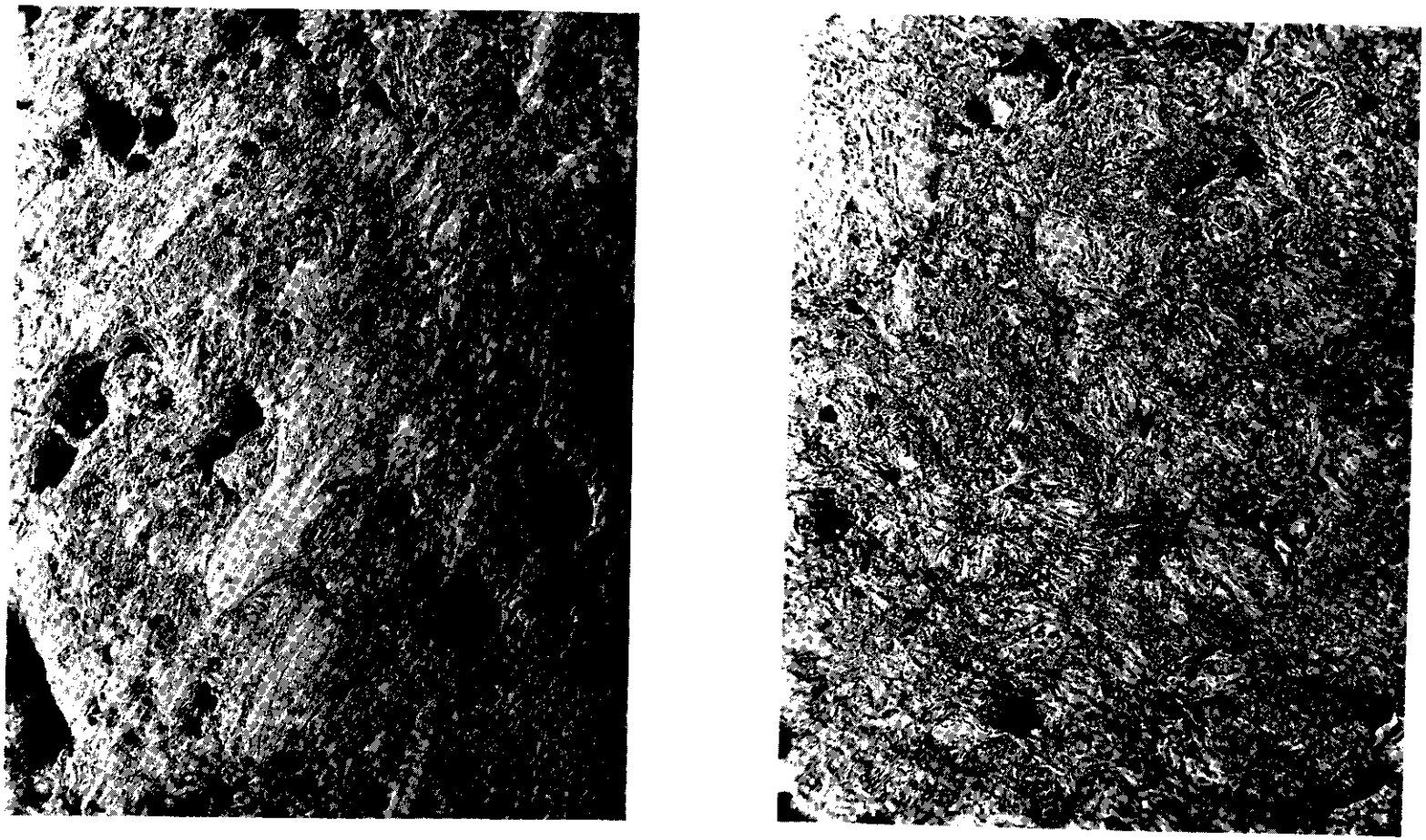

With Grain

Across Grain

Figure 23. Microstructure of Grade ZTF Graphite

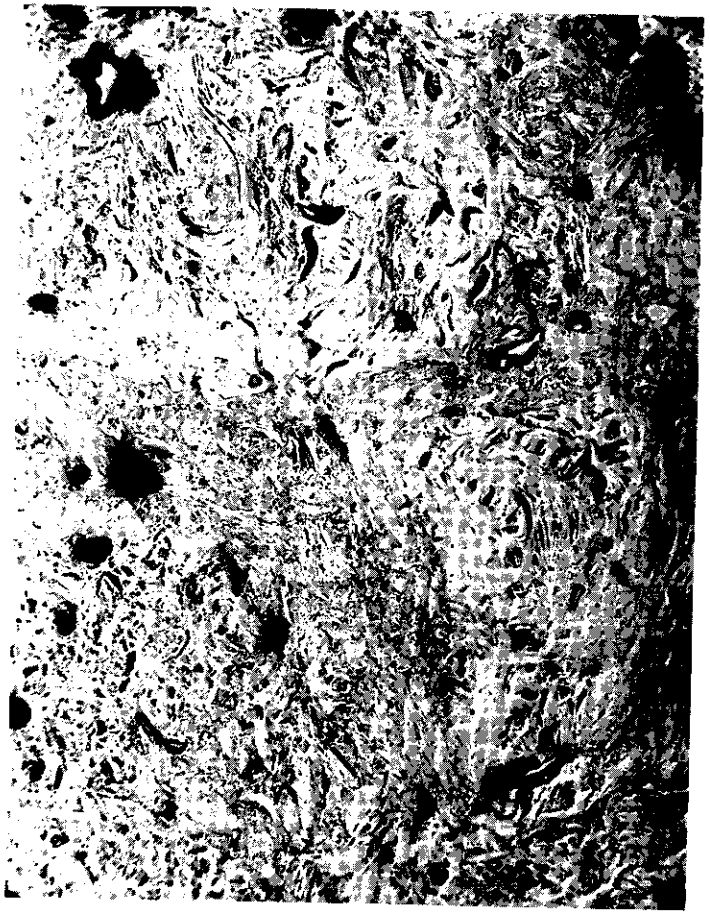

With Grain

Across Grain

Figure 24. Microstructure of Grade CFZ Graphite

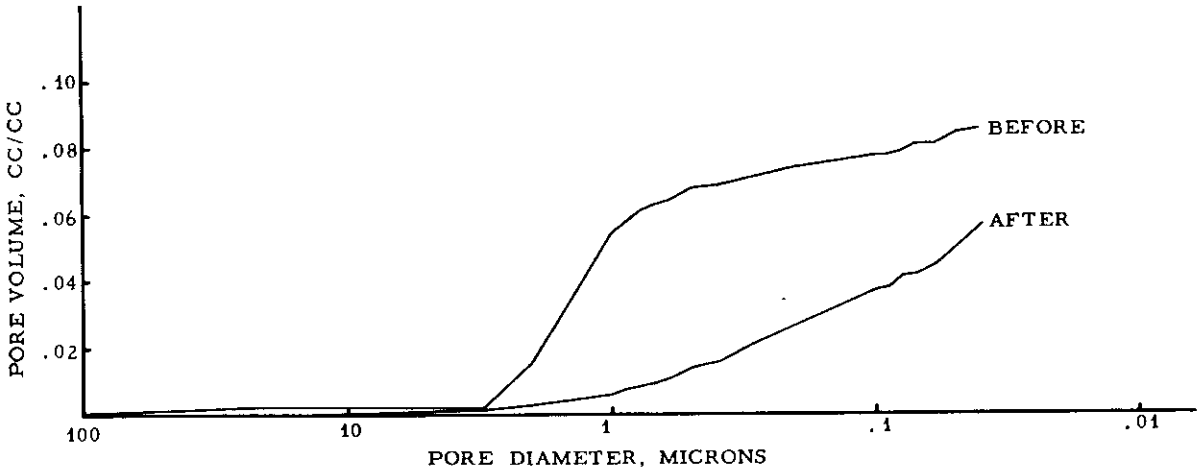

Figure 25. Porosimetry of Grade CFZ Graphite Before and After Hot Pressing

4.3. Hot Pressing of Grade RVD Graphite

Grade RVD[6] graphite made by the pressure-curing process, is somewhat similar to grade ATJ, having nearly the same grain size and similar strengths. The RVD, however, is more anisotropic and is higher in density. Because of this higher density, the RVD has lower porosity than does the ATJ graphite. Figure 26 is a photomicrograph of RVD in the with-grain and across-grain directions. No large pores or individual particles are evident in these photographs, but the overall texture presented appears coarser than does that of the grade ATJ. Both types of materials are made from all-flour blends, but the flour sizing is coarser for the RVD. The photographs show little orientation of the grain structure. The lower porosity also can be seen in Figure 27. There are practically no pores greater than 3 microns in diameter. Almost half the pore volume, which is about 9 per cent, falls in this range, while the remaining half is in pores of less than .09 micron in diameter. The physical properties of RVD are presented in Table 11. Comparison of the properties in the above-mentioned table with those in Table 2 (Physical Properties of ATJ and ZTA Graphites) emphasizes the similarity of the two materials but shows that RVD has higher density and greater anisotropy than grade ATJ.

The one piece of RVD that was successfully hot pressed had a bulk density of 2.045 g/cc, and, as might be expected, had a high degree of anisotropy. The porosimetry curve for the hot-pressed RVD (Figure 27) is much like that of ZTB, having a total porosity of about 3 per cent, with a fractionally higher pore volume along the complete range from 10 to .04 microns. Photomicrographs (Figure 28) show that the hot-pressed RVD is similar to ZTB (Figure 11); however, fewer large pores and much greater alignment, especially in the across-grain photograph, can be seen in the hot-pressed RVD than in the ZTB. The slightly larger flour size used in the RVD is also evident.

With Grain

Across Grain

Figure 26. Microstructure of Grade RVD Graphite

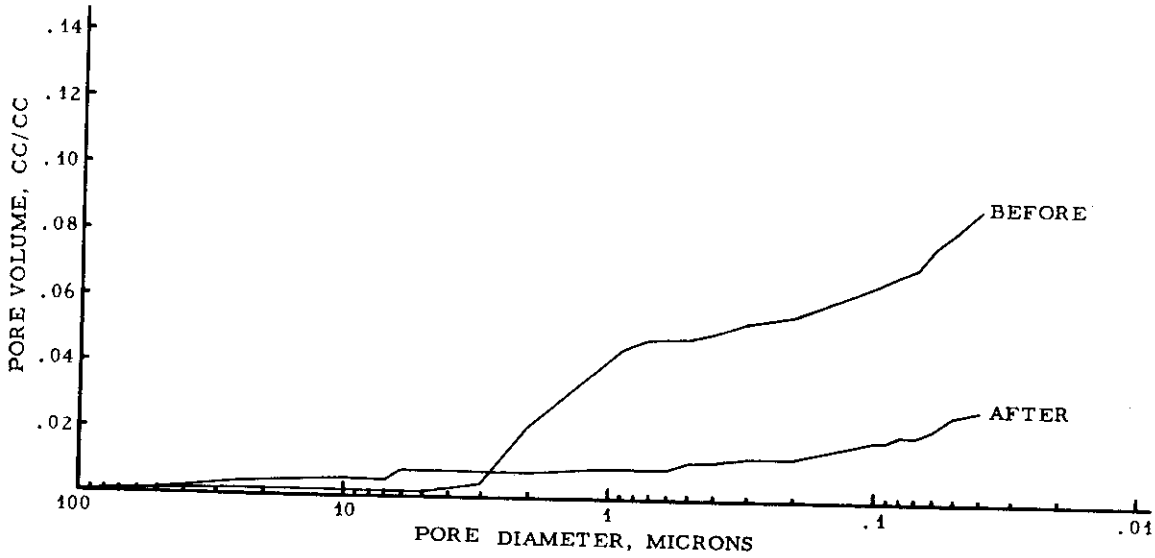

Figure 27. Porosimetry of Grade RVD Graphite Before and After Hot Pressing

Table 11. Physical Properties of Grade RVD Graphite Before and After Hot Pressing

Property		RVD	RVD/ZT
Bulk Density		1.87	2.045
Specific Resistance	w.g.	12.62	6.62
	a.g.	21.64	51.6
Young's Modulus	w.g.	2.10	4.658
	a.g.	1.12	0.540
Tensile Strength	w.g.	4095	
	a.g.	2705	
Compressive Strength	w.g.	11610	
	a.g.	12400	
Flexural Strength	w.g.	4705	
	a.g.	3125	
CTE	w.g.	1.7	-3.0
	a.g.	3.4	+119.9
Thermal Conductivity	w.g.	0.273	
	a.g.	0.198	
Admittance	w.g.	3×10^{-3}	
	a.g.	2×10^{-3}	
CTE(R.T. to 2400°C)	w.g.		27.3
	a.g.		166.1

With Grain

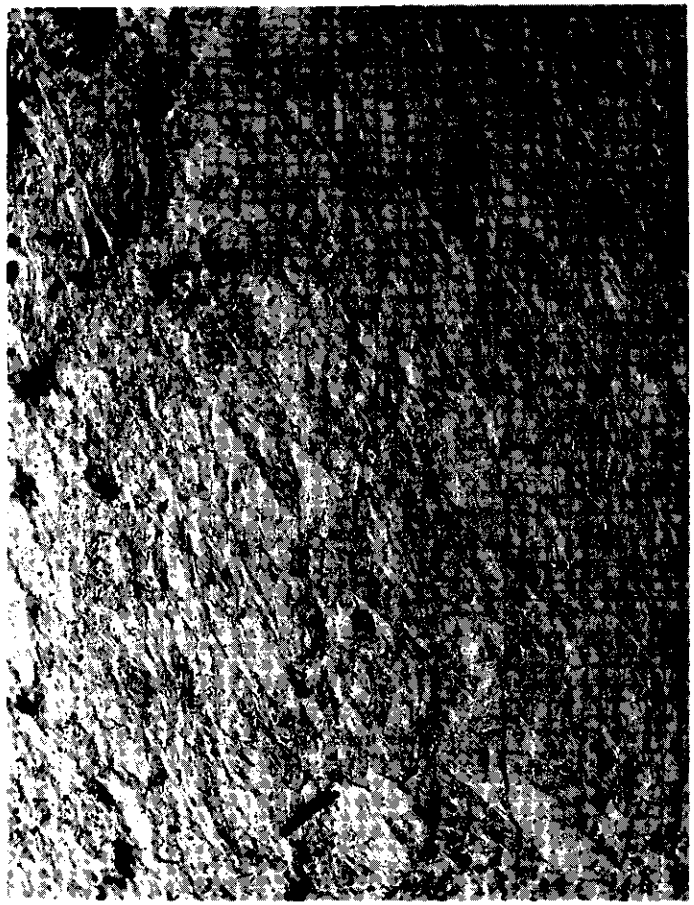

Across Grain

Figure 28. Microstructure of Grade RVD/ZT Graphite

Table 11 shows the physical properties of the hot-pressed RVD. Its most unusual property is its negative value for room-temperature CTE. The anisotropy is so great that the material contracts in the with-grain direction during heating from room temperature to 100°C. Specific resistance and Young's modulus also indicate extreme anisotropy.

4.4. Hot Pressing of Grade RVC Graphite

Grade RVC[7] is a pressure-cured graphite having spherical particles in the blend. Use of these spherical particles prevents alignment, or ordering, of the particles during the forming process, raises the with-grain CTE, and results in a nearly isotropic material. Figure 29 shows photomicrographs of both grain directions of RVC. Several of the spherical particles with their characteristic semicircular voids can be seen in these photographs. The dark-grey area in the lower left-hand portion of the with-grain photograph is not part of the sample but is a section of the mounting styrene.

Grade RVC, in addition to being nearly isotropic in properties (see Table 12), shows high values for density, compressive strength, and CTE, and a total porosity of just over 8 per cent. In Figure 30 it can be seen that the shape of the porosimetry curve is much like that of ATJ graphite. Although total porosity is not high, the greater portion of the pore volume is in pores of larger than 1 micron in diameter, and more than half of the total pore volume is in pores larger than 4 microns.

Table 12. Physical Properties of Grade RVC Graphite Before and After Hot Pressing

Property		RVC	RVC/ZT
Bulk Density		1.85	2.00
Specific Resistance	w.g.	13.08	8.49
	a.g.	16.40	21.53
Young's Modulus	w.g.	1.77	2.535
	a.g.	1.38	0.845
Tensile Strength	w.g.	2730	
	a.g.	1300	
Compressive Strength	w.g.	11160	
	a.g.	10940	
Flexural Strength	w.g.	3215	3928
	a.g.	2040	1631
CTE	w.g.	3.7	1.3
	a.g.	4.5	8.9
Thermal Conductivity	w.g.	0.268	
	a.g.	0.236	
Admittance	w.g.	2×10^{-2}	
	a.g.	5×10^{-3}	

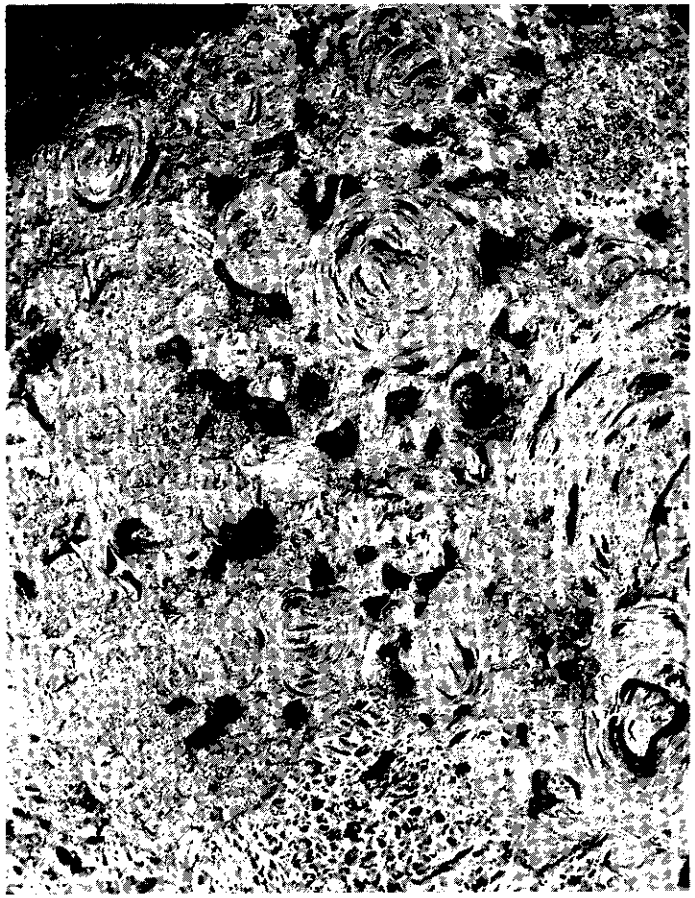

With Grain

Across Grain

Figure 29. Microstructure of Grade RVC Graphite

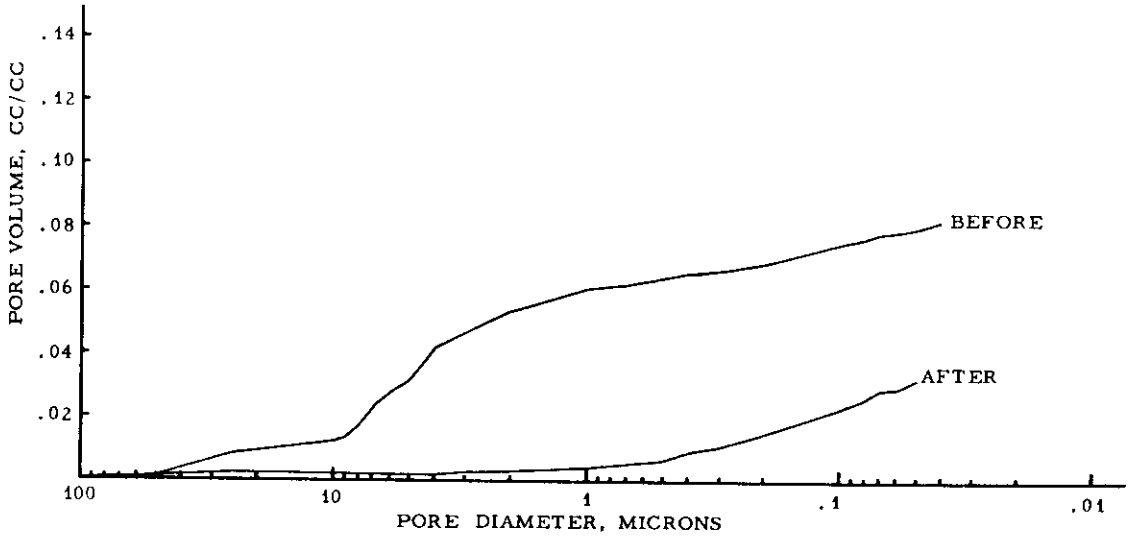

Figure 30. Porosimetry of Grade RVC Graphite Before and After Hot Pressing

The one piece of RVC that was hot pressed and sectioned for physical properties had a final bulk density of 2.00 g/cc with a length reduction of just over 20 per cent. The few properties measured show an unusual combination. Density is equal to that of ZTB, specific resistance, and Young's modulus are what would be expected of ZTA, but flexural strength is about the same as that of CFZ in the with-grain direction and similar to ZTF in the across-grain direction. The across-grain CTE of 8.9 is low for material of this density. Total porosity of the material is about 3 per cent and is similar to ZTB, but, as can be seen in Figure 30, the hot-pressed RVC has a slightly higher volume of pores between 0.5 and 1.05 microns in diameter.

The effect of hot pressing on the spherical particles is shown in Figure 31. What were spheres have now become ellipsoids. There is a reduction in the amount of void space between particles, and the particles themselves appear to have fewer voids. The hot-pressed material, being less porous than the base stock, is more difficult to impregnate with styrene during preparation for photomicrographs, and the pores appear black in the photomicrographs of the hot-pressed material, while they appear grey in the base material (Figure 29)

4.5. Effect of Increased Binder Carbon on Hot-Pressed Graphite

4.5.1. Increased Binder Carbon by Use of Activated Coke in Pressure-Cured Graphite

During the pressure-curing process,[6] changes which occur in the surface area of the inert filler material used in the initial blends are believed to have a large effect on the strength of the resultant piece of graphite. Filler materials with higher surface areas should produce graphites with higher strengths. To test this theory, activated coke particles

With Grain

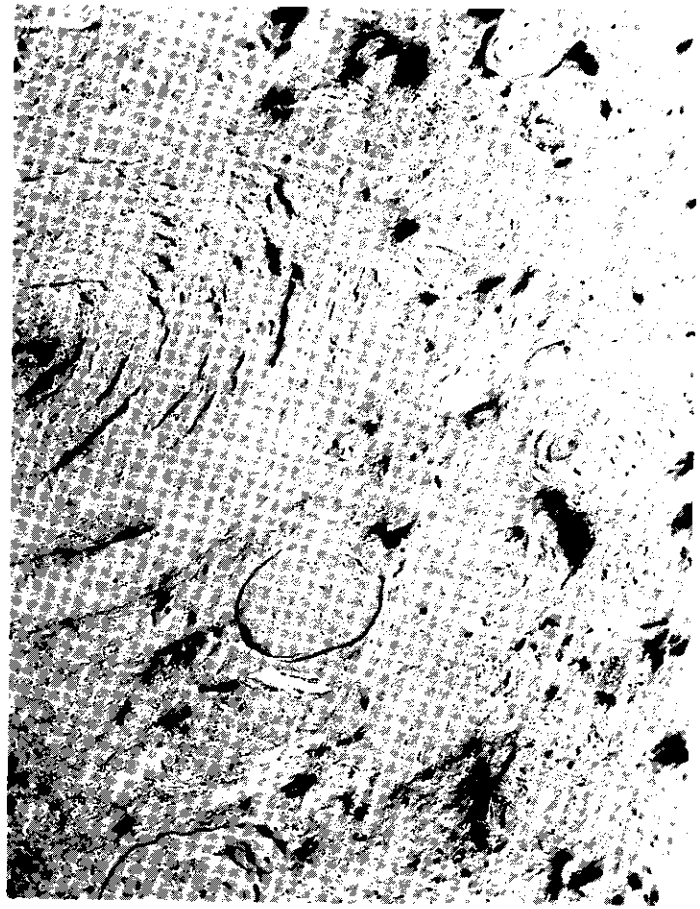

Across Grain

Figure 31. Microstructure of Grade RVC/ZT Graphite

and flour were substituted for some of the graphite filler material used in pressure-curing blends. Since activated coke has a high surface area, increased strengths were anticipated. Hot pressing of such a pressure-cured graphite might produce a graphite with strengths comparable to ZTA and with its other properties comparable to ZTE.

Several 10-inch diameter by 10-inch length plugs, using varying amounts of activated coke and pitch in the blends, were formed by the pressure-curing process. The room-temperature properties of the graphitized plugs are given in Table 13, from which it can be seen that there was no improvement in strength for the various blend combinations tested.

The lack of strength improvement is believed to be due to the high shrinkage of the activated coke which was experienced on graphitizing to 2800°C (see shrinkage data in Table 13). The incompatibility of the coke and graphite filler, as far as shrinkage on heating is concerned, might have caused microflaws to form in graphitization which would result in low strengths, high specific resistance, and cracked stock (particularly where the per cent activated coke was high).

Since the anticipated strength increase was not achieved, none of this material was hot pressed.

4.5.2. Increased Binder Carbon by Use of Preprocessed Inert Filler Material

Preliminary work on ZT processing indicated that the binder carbon content of the graphite used as the starting material had some effect on the strength of the material after ZT processing. Strengths were high when the binder carbon content of the starting material was high (see binder carbon content of grade ATJ and pressure-cured graphite in Table 14).

In an attempt to upgrade the strength, pressure-cured stock was made from an initial blend using inert filler material which contained binder carbon. The inert filler material, which contained 16 per cent thermoset binder carbon, was crushed and milled into particles and flour. Pitch was added to the filler material in the same proportion as used in standard pressure-cured blends, thus increasing the total binder carbon content of the pressure-cured graphite.

The increased electrical resistivity of the blend, caused by the high binder content, resulted in nonuniform temperatures during the resistance heating used in the pressure-curing process. Because of the temperature variation, the pressure-cured pieces formed from this type blend were cracked and the project was discontinued.

4.5.3. Increased Binder Carbon by Impregnation of Porous Material

Increased binder carbon was obtained in pressure-cured stock by making a highly porous graphite base material, impregnating, and rebaking

Table 13. Properties of Graphite Fabricated from Activated Coke

Piece No.	Blend Composition (Parts)							Bulk Density In Cured State	Bulk Density In Baked* State	Per Cent Pitch Impregnation Pickup	Bulk Density In Graphitized State	Per Cent Shrinkage From Bake To Graphite	Flexural Strength**		Electrical Resistivity		Comments
	Graphite Flour	Activated Coke Flour	Graphite Particles	Activated Coke Particles	Carbon Black	Pitch	Sulfur						w.g.	a.g.	w.g.	a.g.	
1	50	0	0	50	8	26	5.2	1.38	1.35	19.5	1.53	6.6	2440	1030	26.9	38.6	Horizontal crack in center
2	0	50	50	0	8	26	5.2	1.37	1.30	25.5	1.55	9.7	1070	390	24.6	40.1	Horizontal and vertical cracks on surface and center
3	25	25	50	0	8	26	5.2	1.62	1.57	10.3	1.70	7.1	3330	2300	14.8	20.7	Horizontal and vertical cracks on surface and center
4	50	0	25	25	8	26	5.2	1.61	1.55	9.2	1.67	7.1	3420	2490	17.3	24.8	Piece flaw free
5	50	0	25	25	8	26	5.6	1.61	1.59	8.0	1.73	8.9	3180	2360	15.4	21.5	Piece flaw free
6	50	0	25	25	8	30	6.0	1.61	1.60	7.6	1.74	9.4	3190	2440	14.8	20.4	Piece flaw free
7	50	0	25	25	8	32	6.4	1.62	1.60	6.8	1.75	9.9	3520	2480	15.1	20.5	Piece flaw free
RVA	50	0	50	0	8	26	5.2	1.79	1.77	5.3	1.82	3.8	3530	2560	11.3	16.5	Piece flaw free

* Baked to 800°C

** ½- by ½-inch Cross Section, Third-Point Loading

Table 14. Binder Carbon Content and Strengths of Grades ZTA, ATJ, ZTE and RVA Graphite

Grade Material	Weight % Binder Carbon Content	Bulk Density	Tensile Strength		Flexural Strength	
			w. g.	a. g.	w. g.	a. g.
ZTA	-	1.95	4380	1510	5500	2350
ZTA Base Stock (ATJ)	40	1.73	3160	2950	5632	4006
ZTE	-	1.96	3210	1470	4340	2315
ZTE Base Stock (RVA)	20	1.85	2800	2160	3700	2880

one or more times. The use of two impregnations appreciably increased the strengths, but when more than two impregnations were used the stock cracked on rebake. Properties of the stock, with one and two impregnations, are listed in Table 15.

Table 15. Physical Properties of Impregnated Highly Porous Graphite

No. of Impregnations	Forming Pressure	Bulk Density	Flexural Strength		Specific Resistance		Young's Modulus	
			w. g.	a. g.	w. g.	a. g.	w. g.	a. g.
1	600	1.63	1740	1250	12.6	15.4	1.07	0.74
1	1000	1.70	1935	1260	11.3	14.3	1.16	0.76
1	2000	1.75	2130	1100	10.0	14.9	1.32	0.71
2	600	1.72	2450	1930	12.3	15.4	1.34	0.97
2	1000	1.78	2505	1760	10.2	12.9	1.35	0.96
2	2000	1.80	2830	1610	9.8	13.9	1.53	0.90

It was found that initial forming pressure affected the impregnated porous stock. Low forming pressure produced a material with only slightly lower strengths, but with a marked increase in porosity or decrease in bulk density. The effects of forming pressure are also shown in Table 15.

Hot pressing of the porous stock was not successful; each of several pieces was extensively cracked after normal hot working. The reason for cracking is not understood, but a possible cause was overstressing of

the stock due to a difference in CTE between the impregnant and the base material.

In the photomicrograph of the hot-pressed stock (Figure 32), large amounts of impregnant (light-grey areas), and many large pores (dark-grey areas) are evident. Porosity is so great that the material would be unattractive for many uses even if it could be processed successfully.

Figure 32. Microstructure of Impregnated Porous Graphite After Hot Pressing

5. HOT PRESSING OF EXTRUDED GRAPHITES

Two extruded graphites were used in these hot-pressing trials, differing from each other in mix composition. One of these graphites was made from an all-flour mix with a maximum grain size of 0.015 inch; the other was made from a mix containing both flour and particles with a maximum grain size of 0.030 inch. For convenience, these extruded graphites will be referred to, in this report only, as grades "CA" (0.015-inch grain) and "CB" (0.030-inch grain). It was hoped that these extruded graphites, having a low with-grain CTE, would supply a ZT material having a lower degree of anisotropy. Table 16 shows the physical properties of grades CA and CB.

Table 16. Physical Properties of Grades CA and CB Graphite

Property		CA	CB
Bulk Density		1.68	1.72
Specific Resistance	w.g.	8.19	8.60
	a.g.	13.10	11.00
Flexural Strength	w.g.	2810	2400
	a.g.	1320	1970
Tensile Strength	w.g.	1400	1440
	a.g.	-	-
Compressive Strength	w.g.	-	5990
	a.g.	-	5960
Young's Modulus	w.g.	1.78	1.49
	a.g.	0.84	1.11
CTE	w.g.	1.35	2.22
	a.g.	-	3.77
Thermal Conductivity	w.g.	0.377	0.360
	a.g.	0.237	0.282

In hot pressing grade CA the aim of reducing the CTE anisotropy ratio was met, but only by the use of mild hot pressing (length reduction of the billet was 17 per cent) and by using stock that was impregnated before hot pressing. The lowest anisotropy ratio obtained (see Table 17) was 3.13 and this was at a bulk density of 1.87 g/cc. It was found that there were variations in the densities of the CTE samples so that the bulk density of the piece, coupled with the CTE's measured, does not present a true picture. A more factual view was obtained when two pieces, in which the bulk density of the with-grain sample was 1.80 and of the across-grain sample was 1.83, gave a measured CTE ratio of 1.51.

No physical properties, other than porosimetry, were measured for the hot-pressed CB material, but photomicrographs were taken of hot-pressed samples having bulk densities of 1.76 to 1.97 g/cc. The pictures on each end of the density range are shown in Figures 33 and 34.

Figure 35 shows the porosimetry curve of hot-pressed CB at two densities. At the low-density end the material has a total porosity of about 16 per cent of which two-thirds is in pores of diameters between 1 and 0.1 micron and the remaining 15 to 20 per cent is in pores whose diameters are below 0.1 micron. On the other end of this series, the material with a density of 1.97 g/cc has a total porosity of just over 6 per cent, which would be equivalent to ZTA. The hot-pressed CB, however, has less porosity in the 1- to 0.04-micron diameter range than does the ZTA.

Table 17. Physical Properties of Hot-Pressed Grade CB Graphite

Property	PC-1	PC-2	PC-3	PC-4	PC-5	PC-6	PC-7
Bulk Density							
w. g.	1.94	1.84	1.87	1.92			1.936
a. g.	1.94	1.88	1.90	1.99			1.909
Specific Resistance							
w. g.	7.19	9.10	9.47	8.67			
a. g.	14.97	11.18	12.72	23.79			
Young's Modulus							
w. g.	2.12	1.00	1.50	1.99			1.97
a. g.	0.69	0.85	0.76	0.59			0.59
Flexural Strength							
w. g.	3197	2505	2816	2500			3519
a. g.	1150	1767	1778	1112			1455
CTE							
w. g.	0.53	1.23	1.18	0.06	2.44	2.44	
a. g.	8.34	5.49	3.69	9.17			
Bulk Density of CTE Sample							
w. g.	1.93	1.87	1.89	1.96	1.79	1.80	
a. g.	1.91	1.86	1.83	1.99			

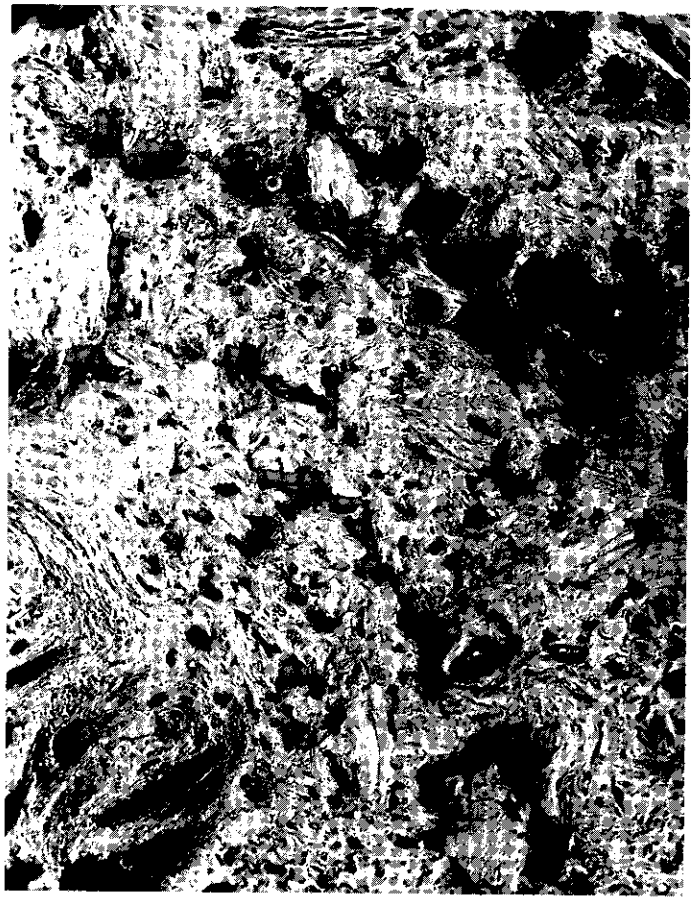

With Grain

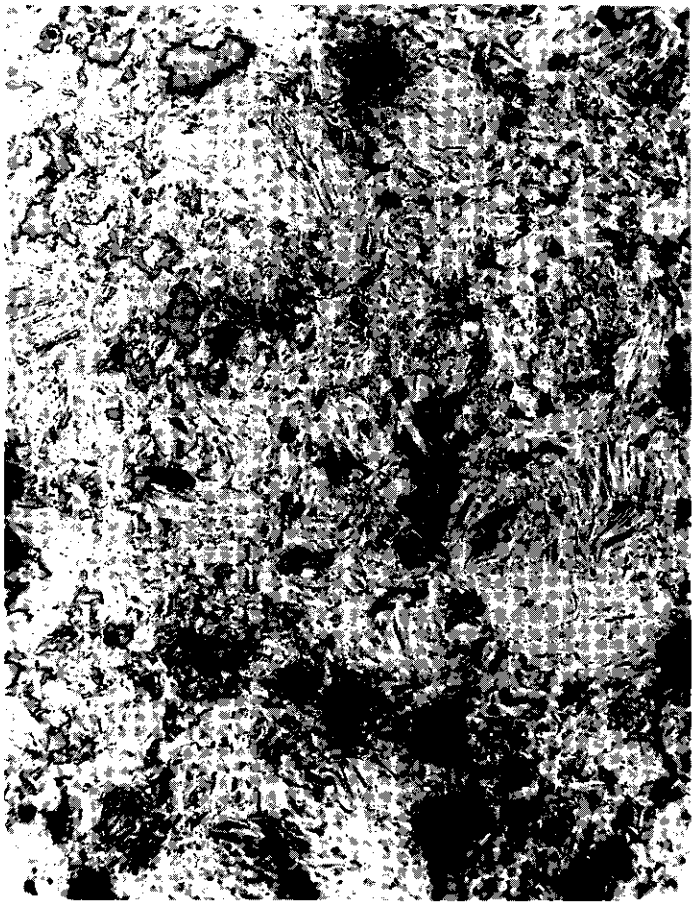

Across Grain

Figure 33. Microstructure of Hot-Pressed Grade CB Graphite, 1.75 g/cc Bulk Density

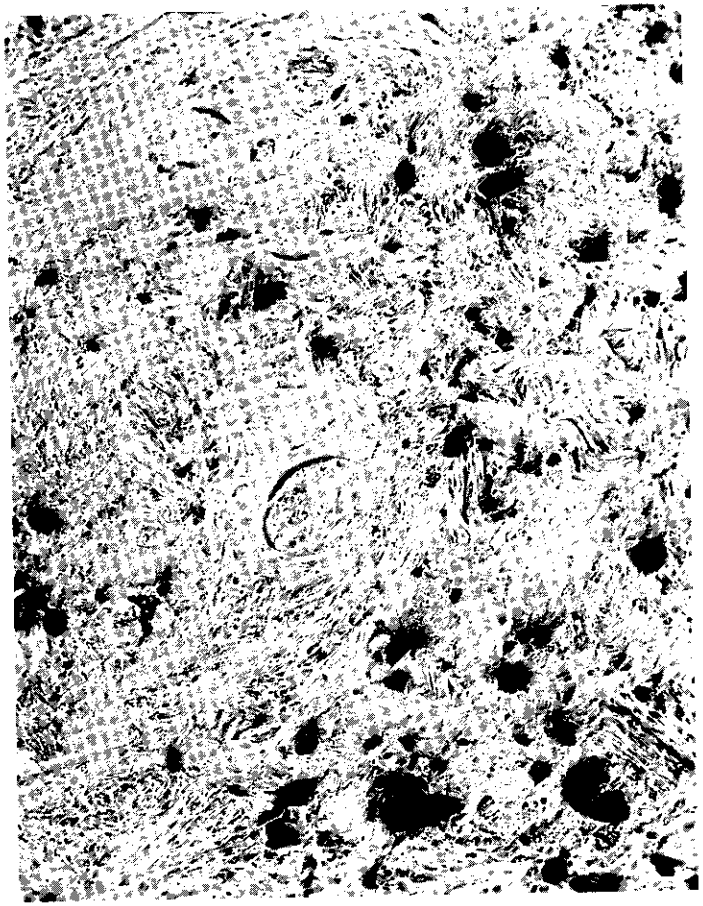

With Grain

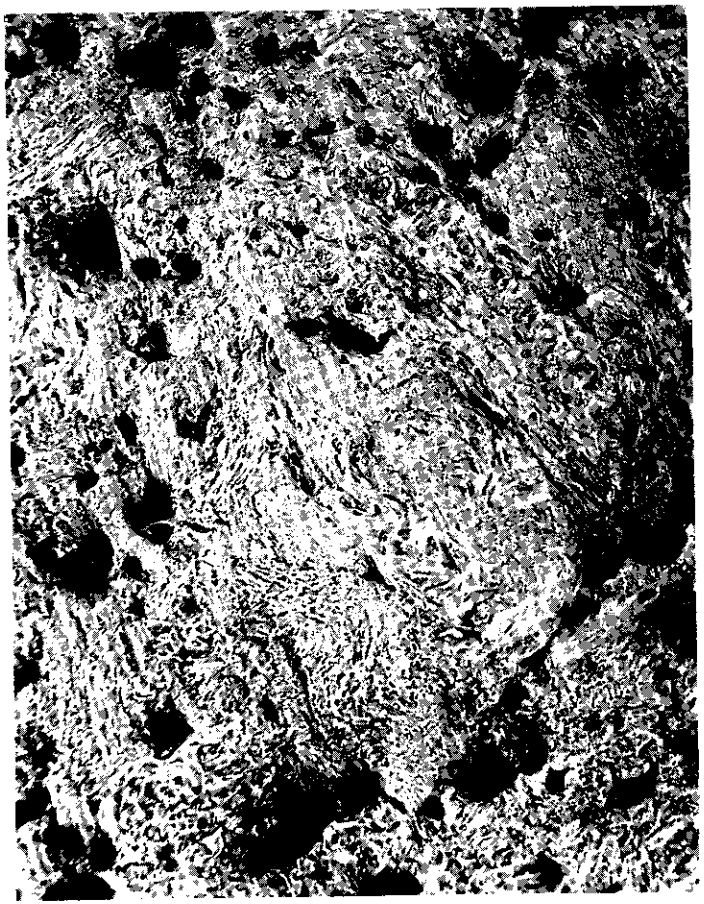

Across Grain

Figure 34. Microstructure of Hot-Pressed Grade CB Graphite, 1.97 g/cc Bulk Density

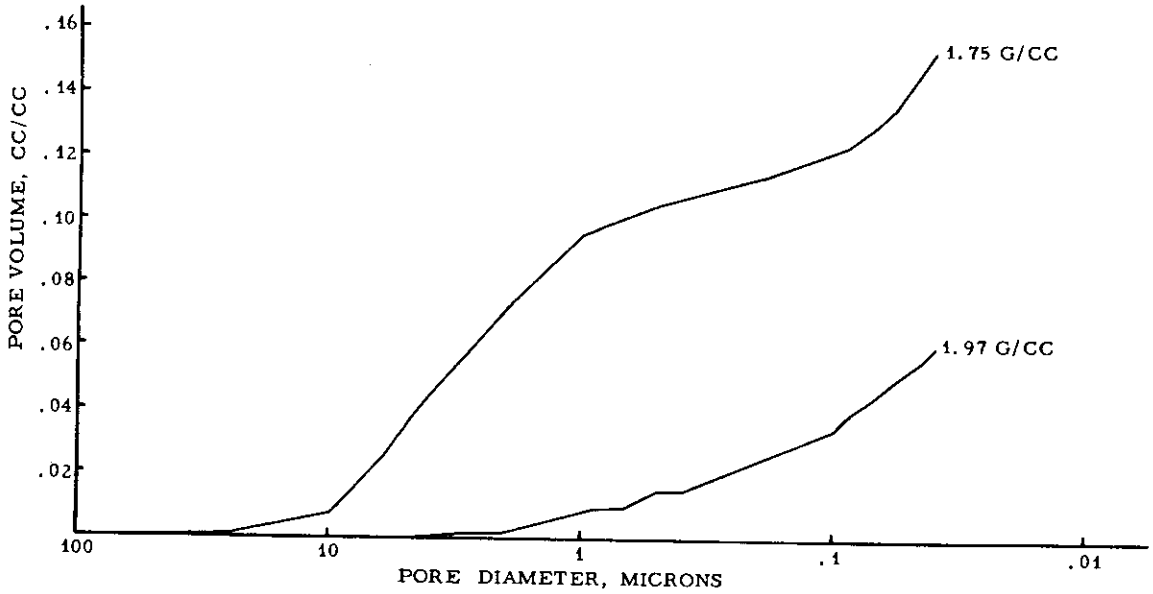

Figure 35. Porosimetry of Hot-Pressed Grade CB Graphite, 1.75 and 1.97 g/cc Bulk Density

6. HOT PRESSING OF POWDERED MATERIALS

Successful hot pressing of powdered blends to a finished high-density product could drastically reduce the processing time for a piece of ZT graphite. Hot pressing of powdered blends has been investigated previously but special cooling was required.[1] The trials discussed herein were made using blends composed of 175°C-melting-point pitch and either powdered coke or powdered graphite. Processing for the blends was almost identical to the hot pressing of solid stock, except that the solid graphite billet ordinarily used was replaced by a cardboard tube filled with blend. Processing time was increased up to 500 per cent over that required for hot-pressing solid stock to allow volatiles given off during heating of the pitch to escape and to compensate for low initial electircal conductivity of the blend. Although pressures used were the same as those in the normal hot-pressing process, the highest density obtained on any of the blocks produced from powdered blends was 1.75 g/cc. This piece had a with-grain specific resistance of 12.71×10^{-4} ohm-cm, a with-grain Young's modulus of 1.208×10^{6} lbs./in.^{2}, and a with-grain flexural strength of 2353 lbs./in.^{2}.

7. DENSIFICATION OF THE SURFACE OF A GRAPHITE ARTICLE BY HOT WORKING

In certain applications, the difference in CTE between the with-grain and across-grain directions of ZT graphite is detrimental. With high ratios of CTE anisotropy, thermal shock resistance of the material is reduced, and circumferential cracking is more likely to occur when the material is used for the nozzle of a rocket motor. On the other hand, the advantage of the ZT material for this application is its high density and low porosity, which results in low erosion rates of the nozzle during firing. One solution to the CTE problem would be to machine the nozzle from graphite having a low CTE anisotropy ratio and then to hot work only that surface which would be exposed to the exhaust gases during firing. This method was used with some success on two pieces of ATJ. The ATJ was in the form of a ring with tapered inside surfaces into which were fitted tapered plungers. The whole assembly was heated until the graphite reached a plastic state, and then the plungers were forced into the ring. This action compressed the inside surface of the ring. Photomicrographs of the ring after hot working show that densification along the inside surface did occur. In Figure 36 it can be seen that one edge of the material has smaller and fewer voids than are found further back in the material. The material near the surface of the ring has the appearance of ZTA with a density of 1.97 or 1.98 g/cc, while the material further back from the surface resembles grade ATJ with a density of 1.73 g/cc. The trials with this surface densification were very limited and no testing was performed in a rocket motor.

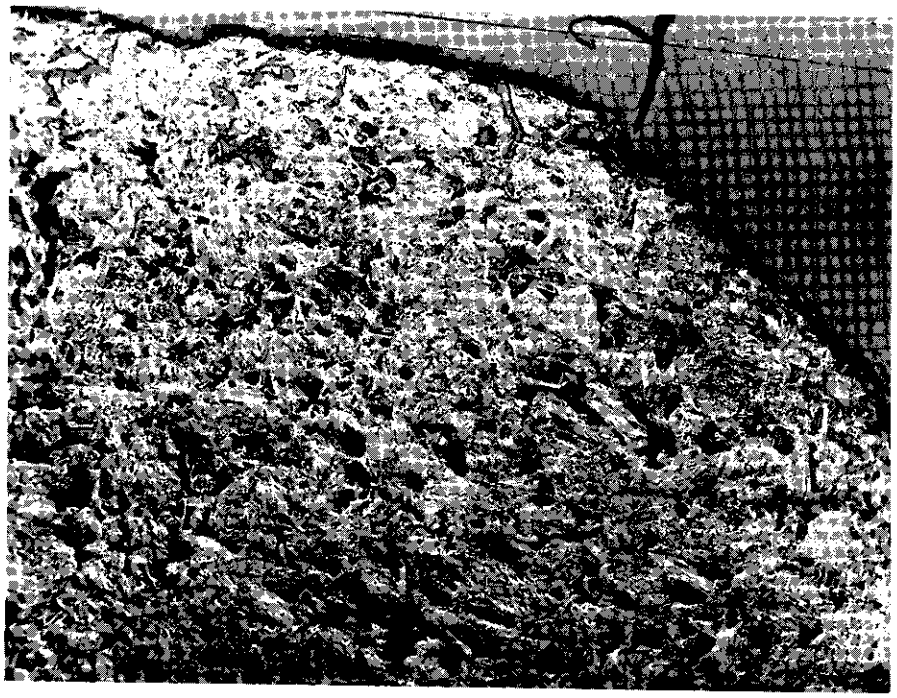

Figure 36. Microstructure of Sample with Hot-Worked Densified Surface

8. HOT PRESSING OF GRAPHITE-REFRACTORY COMPOSITES

The JT family of materials[9] has composites of graphite and additives designed to increase the oxidation resistance of graphite at high temperatures. It was hoped that this material could be prepressed into blocks, and hot pressed to provide a dense, nonporous, oxidation resistant material which would resist erosion during rocket motor firing. The composition of the material used, JT-0854, is shown in Table 18.

Table 18. Composition of Grade JT-0854

	Parts by Weight
BO Graphite Flour	80
175°C-Melting-Point Pitch	20
Sulfur	4
TiB_2	50
Si Powder	18.5
Total	172.5

Theoretical density of this material (assuming 50 per cent coking value for the pitch, no sulfur remaining in the block and all silicon converted to silicon carbide) is 2.85 g/cc. Because of the low binder level, the prepressed blocks of this material were so weak that, on the first hot pressing trial, the block crushed while the press rams were being placed. This was at a pressure of about 1000 lbs./in.^{2}. After nearly 6 minutes of heating, the block deformed rapidly to about 40 per cent of its original length in less than two minutes. At this point heating was discontinued and the pressure was released. Presumably the sudden slump occurred because sufficient additives melted to leave the remaining graphite matrix too weak to support ram pressure. Appearance of the block after hot pressing is shown in Figure 37.

Two methods for reinforcing the stock, both using a graphite constraining ring to provide lateral support, are shown in Figures 38 and 39. In one case, the punch faces covered the constraining ring as well as the stock, and in the other case the punches were intended to go inside the constraining ring. In the first trial with the covered constraining ring, the block began to slump rapidly, decreasing to almost half of its length in less than a minute. In the second trial, with the punches inside the constraining ring, the block again began to slump after 9 minutes of heating, and continued to slump gradually for another 5 minutes of heating time. This latter run with its slow, smooth slump, however, produced the poorest finished material with a density of 1.7 g/cc. The piece which slumped most rapidly had a final density of 2.26 g/cc. Other properties for these materials are found in Table 19.

Figure 37. Photograph of Graphite-Refractory Composite After Hot Pressing

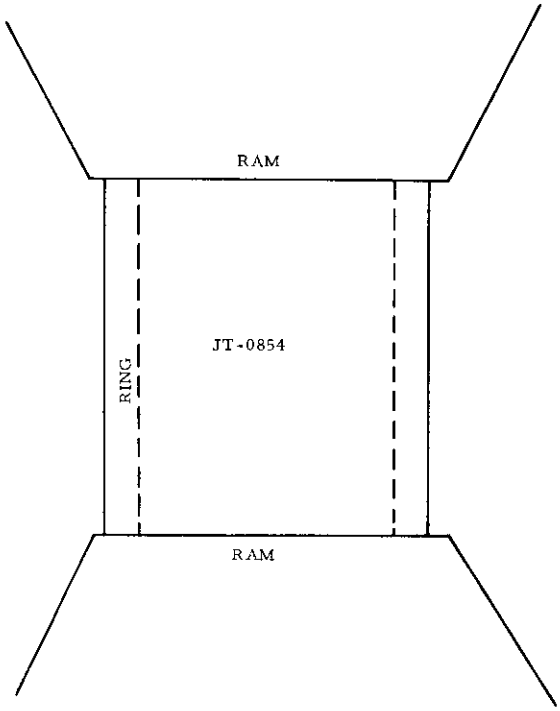

Figure 38. Covered Support Ring for Hot Pressing Graphite-Refractory Composite

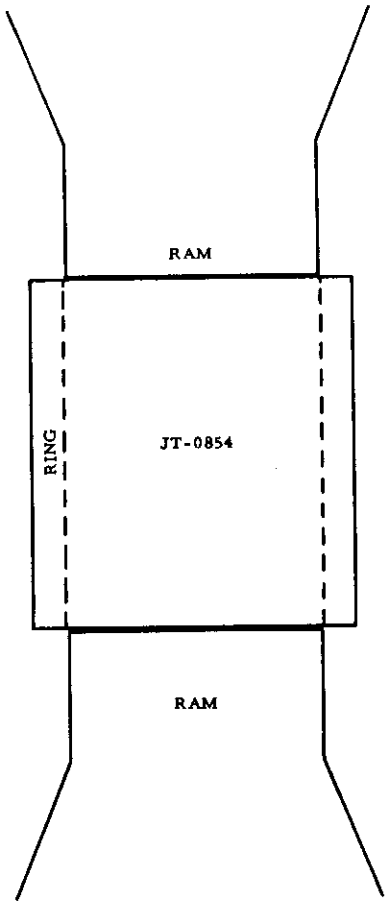

Figure 39. Open Support Ring for Hot Pressing Graphite-Refractory Composite

Table 19. Physical Properties of Grade JT-0854 After Hot Pressing

	Bulk Density	Per Cent Theoretical Density	Specific Resistance	Oxidation Weight Loss, Per Cent, 200 Minutes 800°C	1000°C
No Ring	2.06	72.3	5.00	-	-
Covered Ring	2.26	79.2	4.00	14.39	14.54
Open Ring	1.70	59.7	-	-	-

Figure 40 shows a graphite-refractory composite after hot pressing. One explanation for the behavior in the covered ring might be that the constraining ring, also acting as a heat source to the composite block, allowed the composite materials to become a semimolten mass under comparatively little pressure until the collapse of the ring occurred. At this point the composite block would be subjected to full press pressure, which would cause the rapid slump.

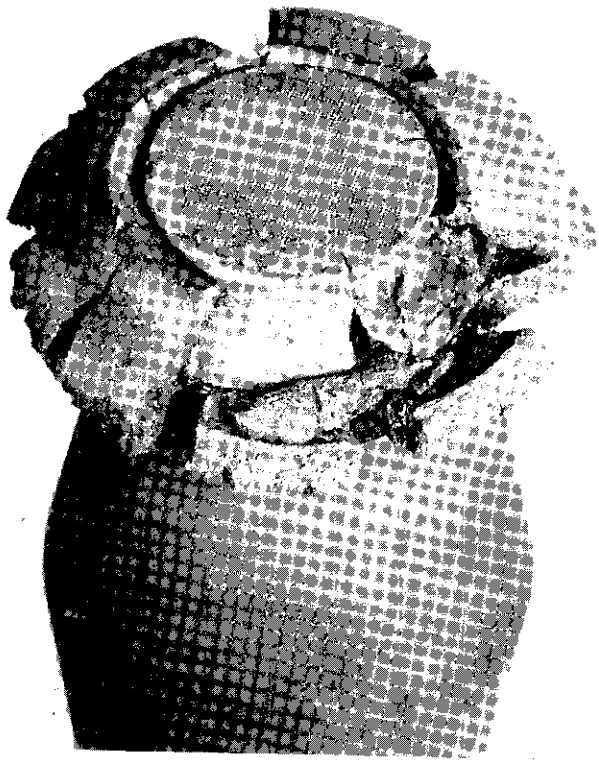

Figure 40. Graphite-Refractory Composite After Hot Pressing in Covered Ring

Samples of JT-0854, JT-0832 (a composite material with silicon and zirconium diboride), and ZTA graphite were exposed to the exhaust gases of a solid propellant, subscale rocket test motor. The JT-0854 sample appeared less oxidized and, after testing for oxidation weight reduction had a weight loss of about half that of the other materials. The weight loss, however, can be somewhat discounted because of differences in sample sizes. Figures 41 and 42 show the oxidation rate (800 and 1000°C) and a porosimetry curve for hot-pressed JT-0854. Total pore volume of hot-pressed JT-0854 is just under 15 per cent (considerably higher than ZTA), with about half the volume taken up in pores greater than 2 microns in diameter. The mercury porosimetry values may be in error, however, because the mercury may wet the composite material to a greater degree than it wets graphite.

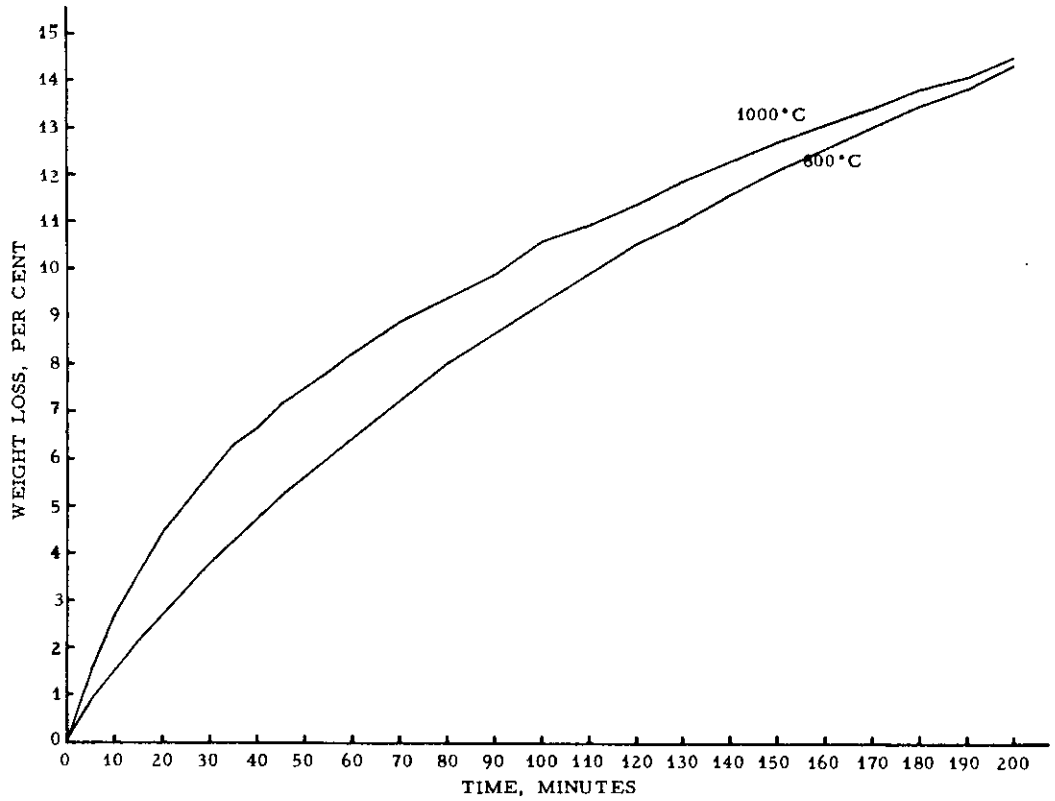

Figure 41. Oxidation of Hot-Pressed Grade JT-0854, 800 and 1000°C

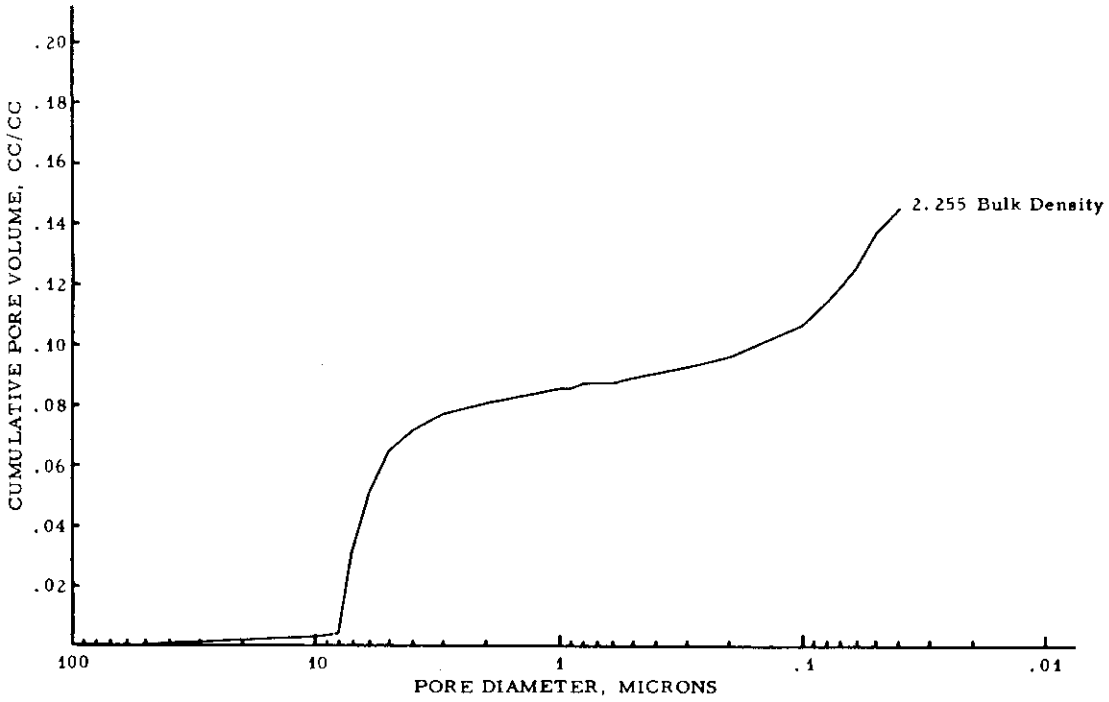

Figure 42. Porosimetry of Hot-Pressed Grade JT-0854

9. SULFUR CONTENT OF INDEX RODS AS A TEMPERATURE INDICATOR FOR THE HOT-PRESSING PROCESS

An attempt was made to use the sulfur content of index rods as a temperature indicator for hot-pressing runs. Index rods are carbon cylinders $^{5}/_{16}$ inch in diameter and $2\frac{1}{4}$ inches in length. Ordinarily they are used, on a one-time basis, as temperature measuring devices (change in electrical resistivity) in electrical furnaces that reach temperatures to 2500°C. During the manufacturing process, index rods retain small amounts of sulfur. As the rods are heated the sulfur is driven off. If the amount of sulfur driven off above 2500°C were appreciable and reasonably linear in temperature dependence, the sulfur content could be used to measure temperature.

To test this possibility, the sulfur content of each of 27 rods baked to a series of temperatures ranging from 1700°C to 3200°C was determined. The rods were packed in the type of coke used in the hot-pressing process and baked in an electric furnace monitored with an optical pyrometer. Figure 43 shows sulfur content of the rods versus baking temperature. From this figure, it is apparent that sulfur content is no better than resistance as a temperature indicator above 2500°C.

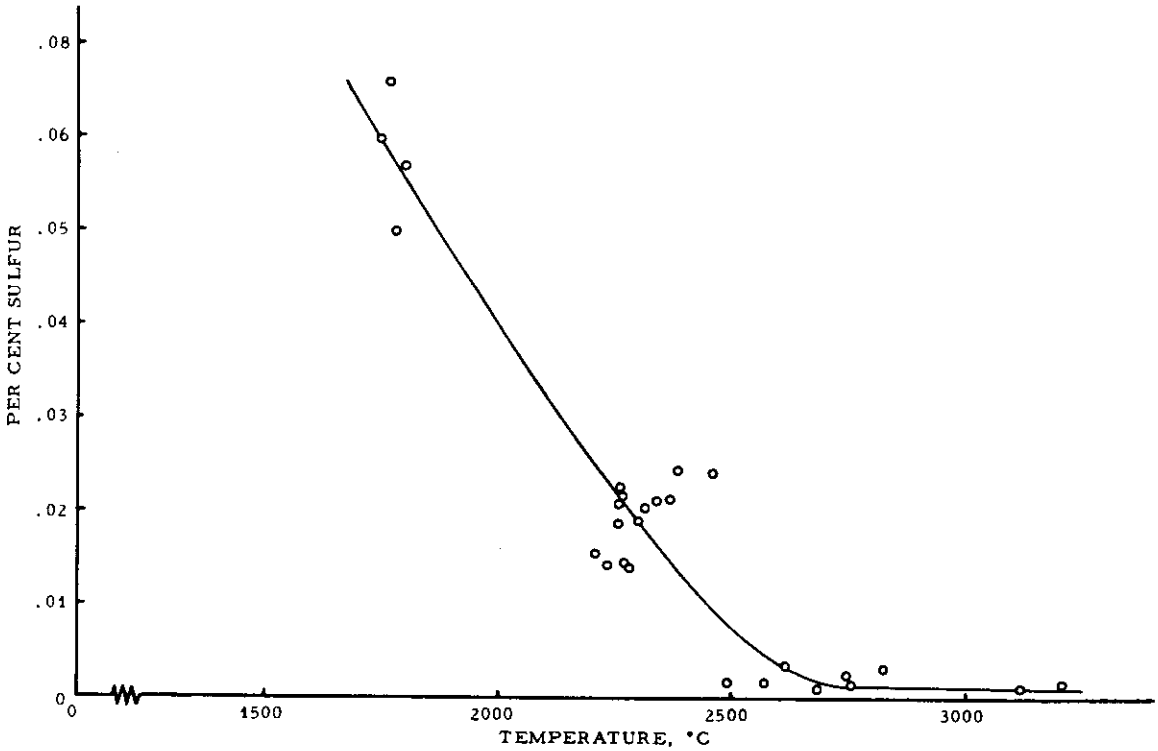

Figure 43. Sulfur Content of Index Rods Versus Final Baking Temperature

10. LIST OF REFERENCES

(1) WADD Technical Report 61-72, Volume VII, "High-Density Recrystallized Graphite by Hot-Forming," by E. A. Neel, A. A. Kellar, and K. J. Zeitsch.

(2) Hill, William J., "Three Short Cuts for Comparing Test Results," Product Engineering (Feb. 15 1960).

(3) WADD Technical Report 61-72, Volume XXXI, "High-Performance Graphite by Liquid Impregnation," by C. E. Waylett, M. A. Spring and M. B. Carter.

(4) WADD Technical Report 61-72, Volume XXXII, "Studies of Binder Systems for Graphite," by T. Edstrom, I. C. Lewis, R. L. Racicot, and C. F. Stout.

(5) WADD Technical Report 61-72, Supplement to Volume VII, High-Density Recrystallized Graphite by Hot-Forming," by G. L. Rowe and M. B. Carter.

(6) WADD Technical Report 61-72, Volume XII, "Development of an Improved Large-Diameter Fine-Grain Graphite for Aerospace Applications," by C. W. Waters and E. L. Piper.

(7) WADD Technical Report 61-72, Volume XXXVIII, "Development of an Improved Large-Diameter Ultrafine-Grain Graphite," by R. A. Howard and R. L. Racicot.

(8) WADD Technical Report 61-72, Volume XIII, "Development of a Fine-Grain Isotropic Graphite for Structural and Substrate Applications," by R. A. Howard and E. L. Piper.

(9) WADD Technical Report 61-72, Volume XXX, "Oxidation-Resistant Graphite-Base Composites," by K. J. Zeitsch and J. M. Criscione.